AD-A063 396 UNITED TECHNOLOGIES RESEARCH CENTER EAST HARTFORD CONN F/G 20/14
FABRICATION OF SPUTTERED ALUMINUM NITRIDE ON SAPPHIRE FOR APPLI--ETC(U)
SEP 78 E L PARADIS, T M REEDER F19628-77-C-0188
UNCLASSIFIED UTRC-R78-922937-4 RADC-TR-78-200 NL

| OF |
AD
A063396

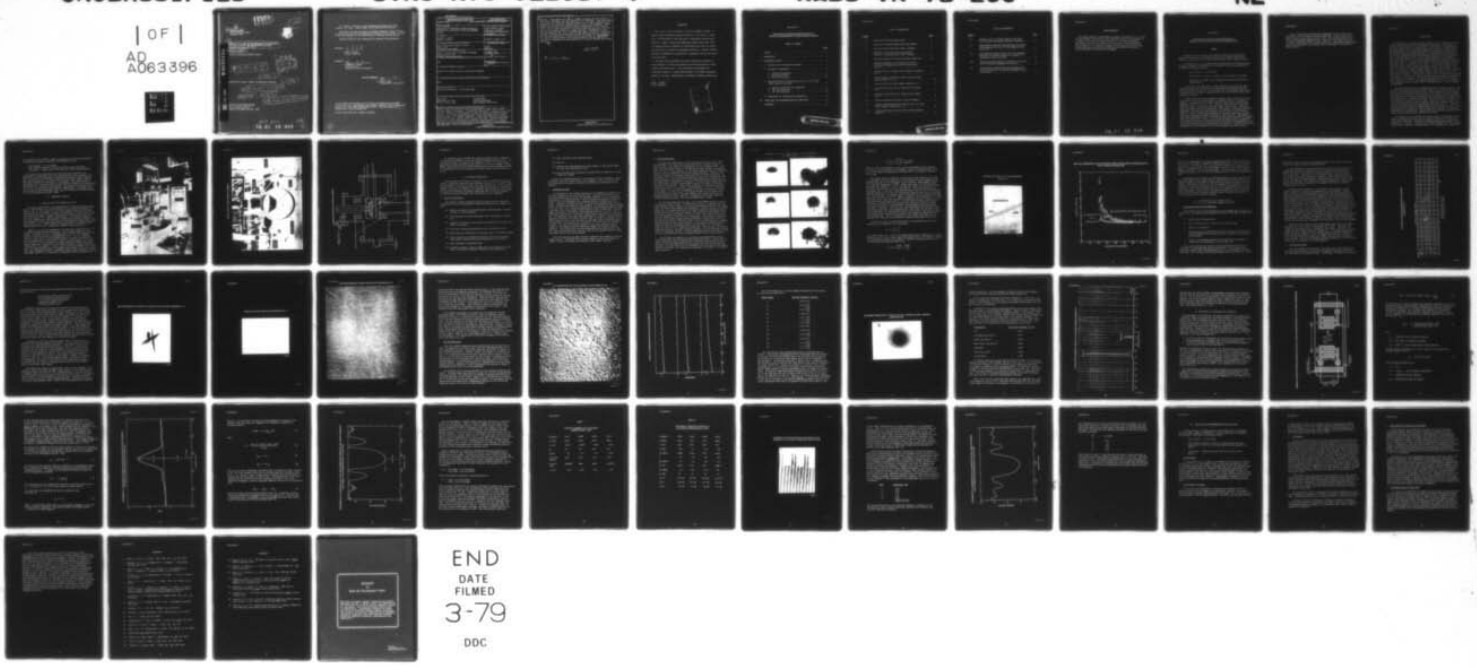

END
DATE
FILMED
3-79
DDC

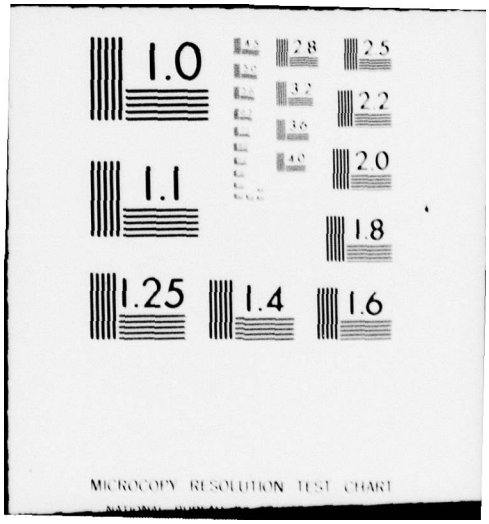
1.0
1.1
1.25
1.4
1.6
2.8
2.5
2.2
2.0
1.8
MICROCOPY RESOLUTION TEST CHART

LEVEL II

12

(18) (19) RADC-TR-78-207
Final Technical Report
September 1978

(6) FABRICATION OF SPUTTERED ALUMINUM NITRIDE ON SAPPHIRE FOR APPLICATION IN UHF SAW FREQUENCY FILTERS.

(10) Edouard L./Paradis
Thomas M./Reeder

United Technologies Research Center

(9) Final technical rept.
1 Jul 77-1 Jun 78,

(11) Sep 78

(12) 58p.

(15) F19628-77-C-0188

(16) 4600 (17) 17

(14) UTRC-R78-9229374

ROME AIR DEVELOPMENT CENTER
Air Force Systems Command
Griffiss Air Force Base, New York 13441

409 252 JRB

Mr. Edouard L. Paradis is the responsible investigator for this contract. Dr. John J. Larkin (ESM), is the RADC Project Scientist.

This report has been reviewed by the RADC Information Office (OI) and is releasable to the National Technical Information Service (NTIS). At NTIS it will be releasable to the general public, including foreign nations.

RADC-TR-78-200 has been reviewed and is approved for publication.

APPROVED: John J. Larkin

JOHN J. LARKIN
Project Scientist

APPROVED: Clarence D. Turner

CLARENCE D. TURNER
Acting Director
Solid State Sciences Division

FOR THE COMMANDER: John P. Huss

JOHN P. HUSS
Acting Chief, Plans Office

If your address has changed or if you wish to be removed from the RADC mailing list, or if the addressee is no longer employed by your organization, please notify RADC (ESM) Hanscom AFB MA 01731. This will assist us in maintaining a current mailing list.

Do not return this copy. Retain or destroy.

UNCLASSIFIED

SECURITY CLASSIFICATION OF THIS PAGE (When Data Entered)

REPORT DOCUMENTATION PAGE		READ INSTRUCTIONS BEFORE COMPLETING FORM
1. REPORT NUMBER RADC-TR-78-200	2. GOVT ACCESSION NO.	3. RECIPIENT'S CATALOG NUMBER
4. TITLE (and Subtitle) FABRICATION OF SPUTTERED ALUMINUM NITRIDE ON SAPPHIRE FOR APPLICATION IN UHF SAW FREQUENCY FILTERS		5. TYPE OF REPORT & PERIOD COVERED Final Technical Report 1 Jul 77 - 1 Jun 78 6. PERFORMING ORG. REPORT NUMBER R78-922937-4
7. AUTHOR(s) Edouard L. Paradis Thomas M. Reeder		8. CONTRACT OR GRANT NUMBER(s) F19628-77-C-0188
9. PERFORMING ORGANIZATION NAME AND ADDRESS United Technologies Research Center Silver Lane East Hartford CT 06108		10. PROGRAM ELEMENT, PROJECT, TASK AREA & WORK UNIT NUMBERS 62702F 46001723
11. CONTROLLING OFFICE NAME AND ADDRESS Deputy for Electronic Technology (RADC/ESM) Hanscom AFB MA 01731 Monitor/John Larkin/ESM		12. REPORT DATE September 1978 13. NUMBER OF PAGES 58
14. MONITORING AGENCY NAME & ADDRESS(if different from Controlling Office) Same		15. SECURITY CLASS. (of this report) UNCLASSIFIED 15a. DECLASSIFICATION DOWNGRADING SCHEDULE N/A

16. DISTRIBUTION STATEMENT (of this Report)

Approved for public release; distribution unlimited.

17. DISTRIBUTION STATEMENT (of the abstract entered in Block 20, if different from Report)

Same

18. SUPPLEMENTARY NOTES

RADC Project Engineer: John Larkin (ESM)

19. KEY WORDS (Continue on reverse side if necessary and identify by block number)

AlN films	rf sputtering
Piezoelectric films	reactive sputtering
Single crystal films	high frequency SAW filters

20. ABSTRACT (Continue on reverse side if necessary and identify by block number)

Single crystal AlN films were grown by sputtering on single crystal (0001) oriented sapphire substrates. The substrate size was 25.4 x 9.0 x 2.0 mm. This size was chosen as a convenient size for the fabrication of UHF SAW frequency filters. The AlN was synthesized by reactive rf diode sputtering of a pure aluminum target in an ammonia atmosphere. Growth conditions were established which yielded clear, uniform, single crystal AlN films. Films were evaluated through microscopic examinations, interference spectrophotometric thickness measurement and electron channeling and X-ray diffractometer crystallographic

DD FORM 1 JAN 73 1473 EDITION OF 1 NOV 65 IS OBSOLETE

UNCLASSIFIED

SECURITY CLASSIFICATION OF THIS PAGE (When Data Entered)

analysis. Films ranged from 2 μm to 2.3 μm in thickness and were uniform to less than 0.1 μm across the long dimension of the substrate. Films were single crystal with the [0001] AlN direction parallel to the [0001] Al_2O_3 direction. Films were clear and smooth replicating the surface of the substrate. Twelve samples were delivered in accordance with the requirements of this program. Surface acoustic wave interdigital electrode transducers and delay lines were fabricated on samples identical to those delivered. Measurements of delay line performance at 201, 477, and 848 MHz were made to provide an estimate of the basic constants for surface acoustic wave excitation and wave propagation. The effective piezoelectric coupling constant was found to be approximately 0.1% and the surface acoustic wave velocity was near 5730 m/s. Relatively low acoustic propagation loss was observed for all AlN on sapphire delay lines studied.

Al 203

* micrometers

EVALUATION

1. This report is the Final Report on Contract F19628-77-C-0188. It covers research performed during the period of 1 July 1977 to 31 March 1978. The objectives of this work were to investigate reactive sputtering as a means of depositing homogeneous single crystal thin films of aluminum nitride on sapphire; to characterize the films for crystalline perfection, uniformity and thickness variation; to deliver research specimens to RADC/ESM for piezoelectric, propagation velocity and device characterization.

2. The above work established the reactive sputtering technique as a prime candidate for producing aluminum nitride films suitable for high frequency SAW applications. This contributes the knowledge and technology necessary to expand SAW processing to the higher frequencies needed for AF radar, communications, and signal processing applications.

JOHN J. LARKIN
Project Engineer

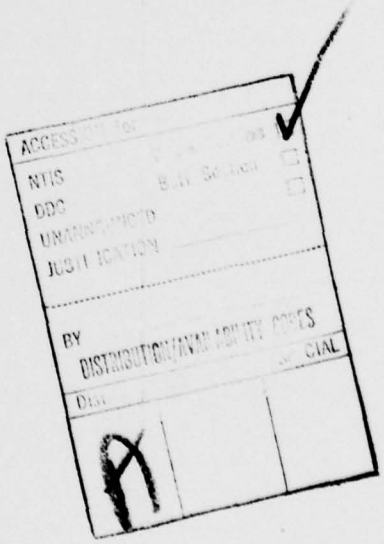

Fabrication of Sputtered Aluminum Nitride on Sapphire for Application in UHF SAW Frequency Filters

TABLE OF CONTENTS

LIST OF ILLUSTRATIONS

LIST OF ILLUSTRATIONS

ACKNOWLEDGEMENTS

The authors gratefully acknowledge the valuable assistance of L. C. Allen, who participated in all phases of the technical portion of this program, of J. Knecht for the electron channeling work, of D. Tucker for electron microscope work, and of D. Moroz for the x-ray work. Additional thanks are extended to R. A. Wagner who oversaw the fabrication of 477 MHz transducers and delay lines and who provided the high quality fabrication of the 848 MHz sample by projection lithography.

R78-922937-4

Fabrication of Sputtered Aluminum Nitride on Sapphire for Application in UHF SAW Frequency Filters

SUMMARY

Research under this program was directed toward the fabrication and evaluation of reactively sputtered aluminum nitride films on sapphire substrates for application in UHF surface acoustic wave (SAW) frequency filters.

The major goals in this program were to demonstrate that aluminum nitride on sapphire prepared by precision rf sputtering in a reactive gas atmosphere can meet the following criteria:

- film thickness - 2 to 8 microns
- film thickness variation - within 0.1 micron across the specimen
- film quality - single crystal aluminum nitride films with optical surface quality.

In the past, AlN films grown by other methods have required post deposition micro-polishing to improve the texture before metallization patterns could be successfully applied. We have shown that rf sputtering could be used to grow AlN films of equal or superior quality but which did not require post deposition polishing.

Single crystal AlN films ranging in thickness from 2.0 μm to 2.3 μm were produced by rf reactive sputtering from an aluminum target in an ammonia atmosphere. The substrates were (0001) oriented single crystal sapphire whose dimensions were 25.4 x 9.0 x 2.0 mm. Deposition conditions were established which were found to yield clear, uniform, single crystal films. Films were evaluated through microscopic examination, spectroscopic interference thickness measurements and electron channeling and x-ray diffraction crystallographic analysis. Surface acoustic wave interdigital electrode transducers and delay lines were fabricated on samples identical to those delivered. Measurements of delay line performance at 201, 477 and 848 MHz were made to provide an estimate of the basic constants for surface acoustic wave excitation and wave propagation. The effective piezoelectric coupling constant was found to be approximately 0.1% and the surface acoustic wave velocity was near 5730 m/s. Relatively low acoustic propagation loss was observed for all AlN on sapphire delay lines studied.

Twelve samples which satisfied the requirements of the contract were delivered to Air Force RADC for further evaluation. Further work should be done to improve crystal perfection and yield. Some attention should also be given to increasing deposition rate. However, it was demonstrated that rf reactive sputtering could be used to grow thick, high quality single crystal AlN films on substrates of a suitable size for fabrication of UHF SAW frequency filters.

I. INTRODUCTION

The fabrication of aluminum nitride films has been of continuing interest in many laboratories because of the potential usefulness of these films in a variety of solid state device applications. In particular, the preparation of single-crystal films of aluminum nitride and silicon on a common sapphire substrate presents the attractive possibility of integrating acoustic, optic and microelectronic processing functions on a single monolithic substrate. In the past, aluminum nitride films have been fabricated in several different ways. Wauk and Windslow (Ref. 1) used thermal evaporation of aluminum in nitrogen and ammonia gas to produce polycrystalline films suitable for microwave delay line use. Chemical vapor deposition (CVD) was employed by Manasevit and Simpson (Ref. 2) and Duffy, et al. (Ref. 3) to fabricate single-crystal films for surface acoustic wave applications. Noriega, et al. (Ref. 4) presented electrical and optical data on polycrystalline films prepared by dc reactive sputtering in argon-nitrogen mixtures. Rutz, et al. (Ref. 5) reported that polycrystalline switchable memory resistors could be fabricated by rf sputtering in nitrogen. Shuskus, et al. (Refs. 6 and 7) demonstrated that thin-films could be fabricated by reactive sputtering that were equal or superior to those made by CVD techniques. Single crystal films were fabricated in GaAs, $SrTiO_4$, HfO_2, ZnO, and AlN. This program provided the first clear indication that large area, single crystal films of compound materials could be prepared by sputtering.

The basic characteristics of aluminum nitride on sapphire are nearly ideal for the construction of miniature surface acoustic wave (SAW) filters for applications in UHF frequency synthesizers. These filters utilize interdigital electrode structures whose period is equal to the desired acoustic wavelength. The high acoustic velocity of aluminum nitride on sapphire and its moderately large piezoelectric coupling factor allow this structure to be efficiently used at frequencies from 500 to above 1500 MHz. However, attempts to build such filters using aluminum nitride on sapphire fabricated by chemical vapor deposition (CVD) technology have experienced great difficulty (Ref. 8). Films deposited by CVD are relatively rough and must be micropolished in order to allow the application of micron size electrode patterns. Moreover, CVD films have not proved to be reproducible; large material constant variations are seen over single substrates and from one substrate to the next.

The objective of this program was the fabrication by sputtering of high quality aluminum nitride thin films on sapphire substrates of useful solid state device dimensions. Toward this end the substrate size chosen for this program was 25.4 x 9.0 x 2.0 mm and the substrate material was (0001) oriented single crystal sapphire. The major goals in this program were to demonstrate

that aluminum nitride (AlN) on sapphire prepared by rf reactive sputtering in an ammonia gas atmosphere could meet the following criteria:

- film thickness - 2 to 8 microns
- film thickness variation - within 0.1 microns across the sample
- film quality - single crystal AlN films with optical surface quality.

The piezoelectric properties of the AlN films were estimated by the measurement of interdigital electrode, surface acoustic wave transducers and delay lines which were fabricated on samples whose single crystal properties were virtually identical to those of the twelve AlN coated sapphire samples delivered to RADC at the conclusion of the program. These electroacoustic measurements were carried out during a UTRC sponsored program on the experimental characteristics of sputtered film coatings. The results are presented here in the interest of completeness and scientific communication. Additional piezoelectric and acoustic measurements will likely be carried out by RADC personnel on the twelve samples delivered to RADC.

II. EXPERIMENTAL DETAILS

A. Epitaxial AlN Film Deposition System

The growth system used in this program was an rf powered diode sputtering system. A photograph of the system and some of its associated equipment is shown in Fig. 1. The chamber is a six sided stainless steel cross of welded construction and the internal fixturing is fabricated of either stainless steel or nickel plated copper. Flanges and ports on the vacuum chamber are sealed with either vitron A "O" rings or copper gaskets. The system is pumped by a 250 ℓ/sec turbomolecular pump backed by a conventional mechanical roughing pump. Since ammonia is used as the sputtering gas, both pumps are charged with special high stability oils. Chamber pressure is measured with an ionization gauge during pump down and with a capacitance monometer during sputtering.

Figure 2 is a close-up photograph of the sputtering chamber and Fig. 3 is a schematic drawing showing the position of the internal components of the system. The target is a 12.7 cm diameter disk of 99.999 % pure aluminum. The target to substrate distance is approximately 6.4 cm. A 12.7 cm diameter stainless steel shutter is placed midway between the target and substrate to prevent contamination of the substrate during the target sputter clean cycle. The substrate is held and heated by a ceramic coated molybdenum strip heater. Heater temperature is monitored with an optical pyrometer sighted through the viewing port of the chamber. A pair of water cooled electromagnets are located along the target-substrate axis. The magnets are arranged so that their fields add. This arrangement results in reducing substrate surface secondary electron bombardment which in turn contributes to producing a smooth film growth (Ref. 9).

FIG. 1

AlN SPUTTERING SYSTEM

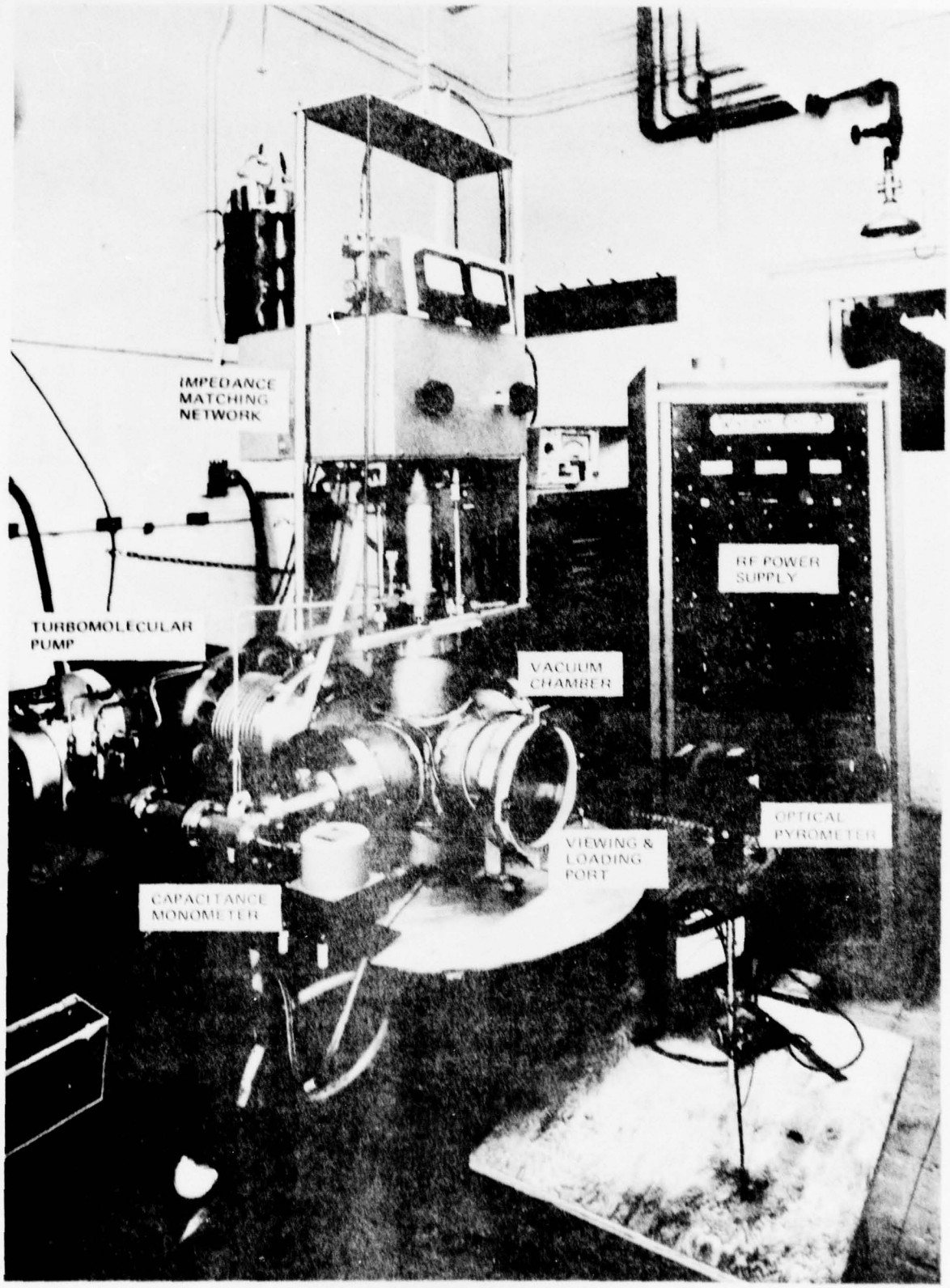

CLOSE–UP OF Al N SPUTTERING CHAMBER

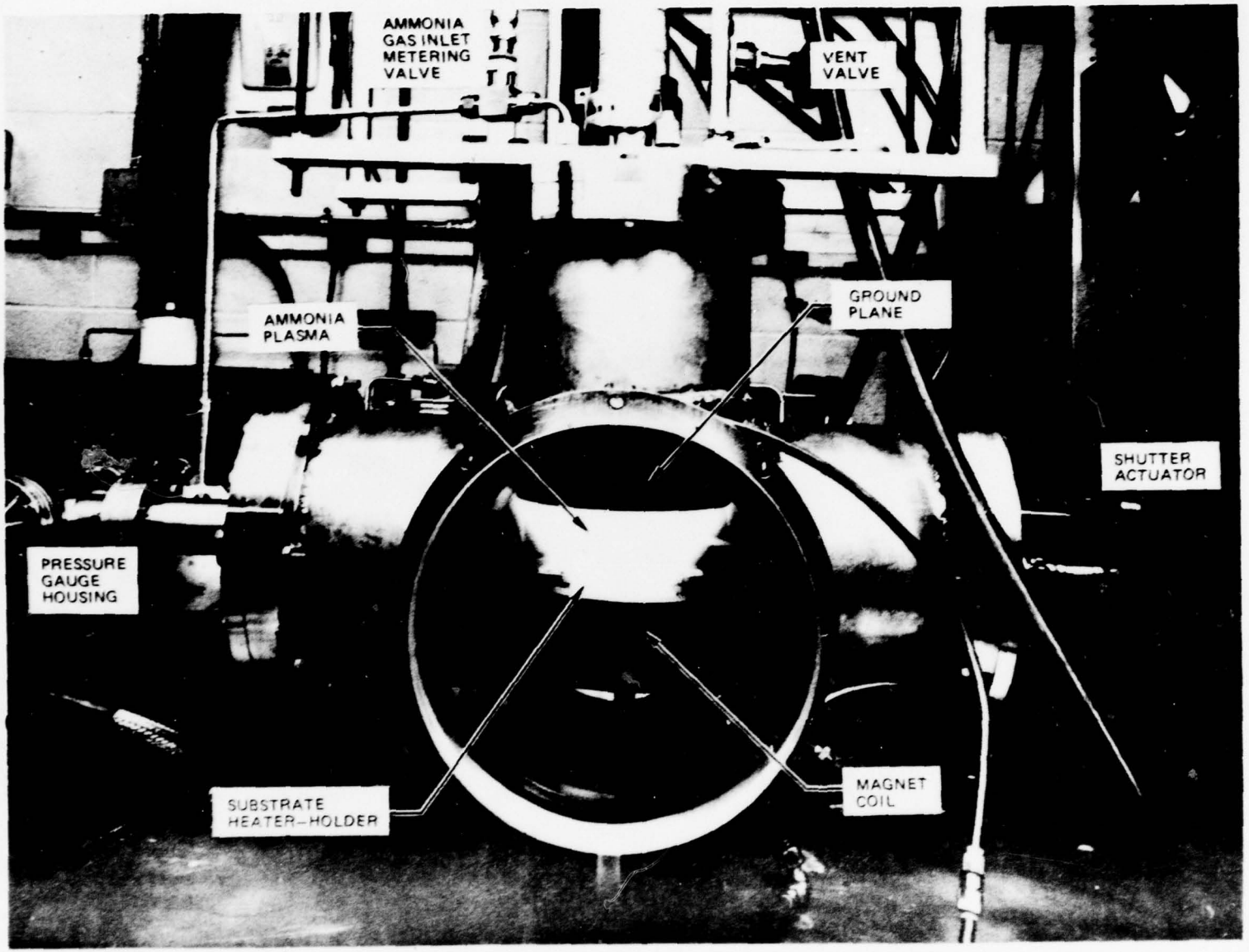

R78-922937-4

FIG 2

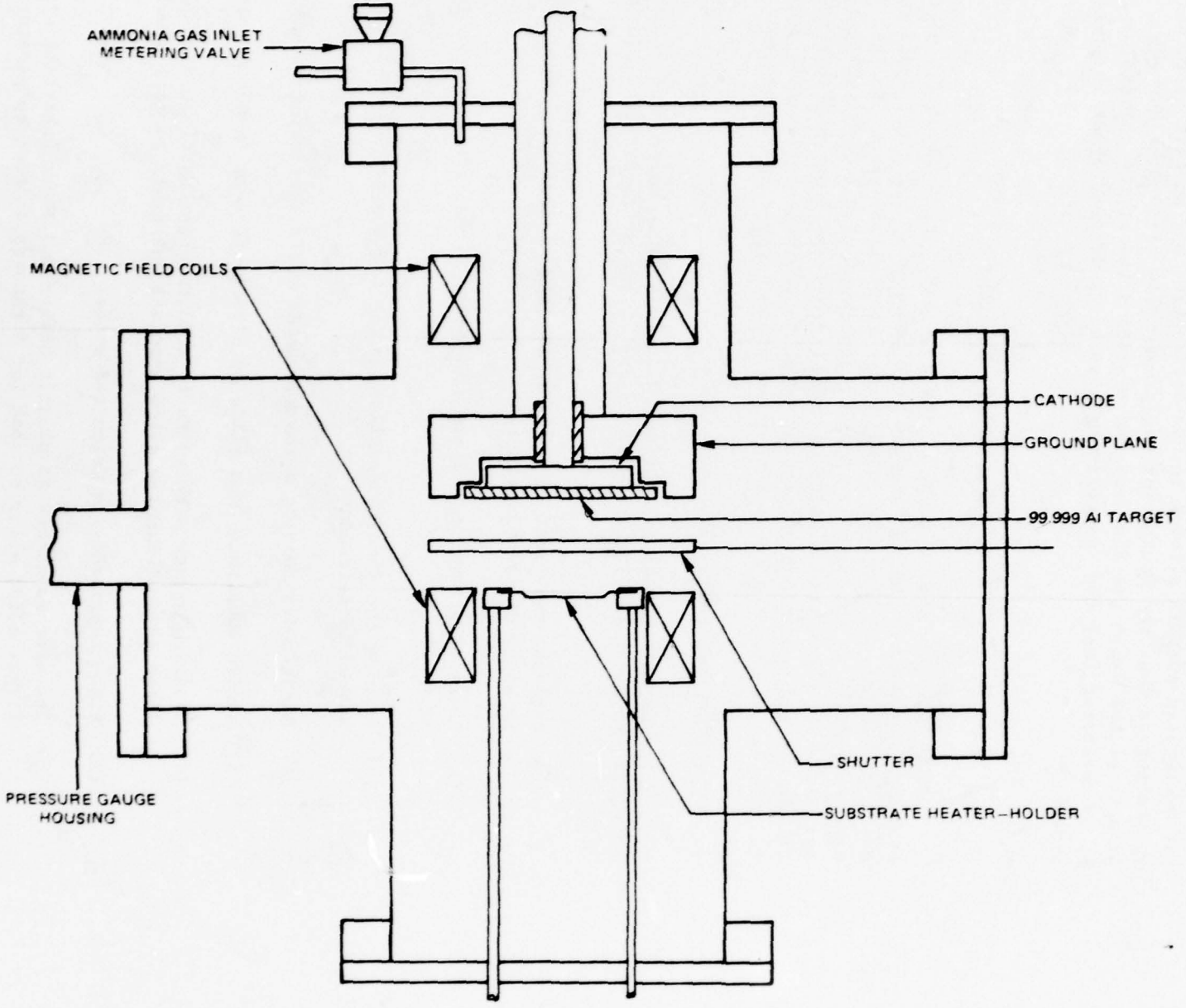

FIG. 3

77-09-110-1

The sputtering gas is 99.999% pure anhydrous ammonia which is admitted to the sputtering chamber through a micrometer adjustment metering valve. The turbomolecular pump is allowed to run unthrottled and at full speed during sputtering so that the sputtering gas pressure is arrived at through a dynamic balance of the inlet gas flow and the pumping speed of the turbomolecular pump. It is estimated that the sputtering gas is being renewed about 10 times per second.

B. Preliminary Experiments

While awaiting the delivery of the 25.4 x 9.0 x 2.0 mm (0001) Al_2O_3 substrates, exploratory deposition runs were made using 6.3 x 6.3 x 0.5 mm (0001) Al_2O_3 substrates which were on hand. This step was important in that we could determine early in the program if major problems existed with the sputtering system. This phase also allowed us to perform a small parametric study around the deposition conditions previously established (Ref. 6) for this process. In this way we would be assured that the process could be reproduced.

1. Substrate Preparation

The substrate cleaning procedure which was found to be most effective consisted of the following sequence of operations performed in a laminar flow hood.

(1) Degrease substrate in boiling MOS grade trichlorethylene. Rinse in in spray of trichlorethylene.

(2) Mount substrate on a glass microscope slide, using soap as an adhesive.

(3) Griping the microscope slide, scrub the substrate with a cotton swab soaked in detergent.

(4) Rinse under running deionized water while continuing to scrub.

(5) Remove substrate from slide by dissolving soap in hot deionized water.

(6) Cover substrate with sulfuric acid and heat until acid is fuming. After several minutes allow acid and substrate to cool slowly.

(7) Rinse repeatedly in deionized water.

(8) Transfer substrate to plastic beaker and cover substrate with hydrofloric acid; allow to soak for 5 minutes at room temperature.

(9) Rinse repeatedly under deionized water.

(10) Spin dry.

(11) Examine under 100X magnification and transport to sputtering chamber in clean covered glass petri dish.

(12) Dust substrate with filtered dry nitrogen blast as substrate is being loaded into chamber.

During the preceeding operation, the substrate is kept submerged in liquid continually from Step 3 until Step 10 is in progress. This is to prevent any air drying and the possibility of water-born residue from depositing on the substrate.

2. Optimization Study

The optimization runs involved variations in the ammonia gas pressure, the substrate temperature, and the deposition rate. Because of the nature of the rf sputtering deposition process, the substrate temperature is not completely independent of the deposition rate. This is because the substrate is partially heated by electron bombardment from secondary electrons originating at the target. Therefore, as deposition rate is increased by increasing power to the target, substrate temperature is also increased. Gas pressure was varied between 0.3 and 4 x 10^{-2} torr. Substrate temperature was varied between 1200°C and 1340° C and power input to the target varied between 6.3 and 7.9 watts/cm^2. The best sample results were obtained at a sputtering gas pressure of 2 x 10^{-2} torr, at a substrate temperature of 1250°C and a power input to the target of 6.3 watts/ cm^2. The deposition rate under these conditions was 70 Å/min. These conditions represent a departure from those previously (Ref. 6) found to yield good AlN on (0001) sapphire films in that the power to the target and the resulting deposition rate had to be reduced from 7.9 watts/cm^2 to 6.3 watts/cm^2 and 100 Å/min to 70 Å/min. The reason for this discrepancy is not clear, although it may be related to the somewhat different sputtering chamber and different internal fixturing. These differences in sputtering geometry were necessitated by the fact that the substrates which were to be used in this program were much larger than those used in the previous program.

The AlN films produced under the above conditions were generally clear and single crystal. Those films which were not single or clear could usually be traced to errors in cleaning the substrate or the chamber fixturing.

3. AlN Film Evaluation

The films were examined for clarity with an optical microscope at 100X, 200X and 500X. Film crystallinity was determined by low angle reflection electron diffraction (RED) in a transmission electron microscope (TEM). However, since the sample chamber of the TEM was not large enough to accommodate the 25.4 x 9.0 x 2.0 mm substrate, it had been decided that electron channeling would be used to evaluate the films on the large substrates. Electron channeling is a method for analyzing crystal structure of films and surfaces. In this method 2 kV to 20 kV electrons impinge the surface to be analyzed at near normal incidence. The electrons that are Bragg reflected near the surface of the sample can be backscatter to a detector. Electrons which channel deep into the film between the atomic planes however have little chance of being backscattered to the detector. This process of elastic and inelastic scattering of electrons results in a pattern of "pseudo-Kikuchi" lines at the detector characteristic of the crystal arrangement of the atoms at or near the surface of the sample. In order to get a correlation between the RED analysis and electron channeling, some of the small samples were examined with electron channeling as well as RED. Figure 4 is a comparison of the RED pattern and electron channeling patterns for three different quality films.

For the polycrystalline film (Fig. 4-A) no discernable pattern is seen in the electron channeling mode. The RED pattern of Fig. 4-B indicates that the film is single crystal, however, the electron channeling pattern for the sample shows only a barely discernable six pointed star. Finally, in Fig. 4-C the RED pattern for this sample shows that it is single crystal of exceptional quality displaying not only a sharp spot pattern but a brilliant set of Kikuchi lines. The electron channeling pattern for Fig. 4-C shows a well defined six pointed star and complex fine structure in the background. Since electron channeling patterns are generated through elastic and inelastic scattering of electrons the same way as Kikuchi lines are in RED, it is not surprising that the samples exhibiting Kikuchi lines in RED would have a good electron channeling pattern. Therefore, electron channeling indicates in a qualitative way the relative quality of the films in a similar way as RED does. Note also that the electron channeling pattern is the same as one would expect for two-dimensional Brillouin zones for a hexagonal lattice. Electron channeling patterns can therefore also be used to determine quantitative information about the AlN crystal lattice.

Film thickness was measured by interference spectrophotometry using a Perkin-Elmer model 202 Ultraviolet-Visible Spectrophotometer. The periodicity of the interference spectrum generated by constructive and destructive interference of the reflections from the film surface and from the film-substrate interface is a known function of the thickness of the film layer in the region exposed to the beam. For a beam with a fixed angle of incidence this relationship is given by

FIG. 4

COMPARISON OF RED WITH ELECTRON CHANNELING PATTERNS OF SPUTTERED AlN ON (0001) SAPPHIRE

RED

A. POLYCRYSTALINE #8-8

e⁻ CHANNELING

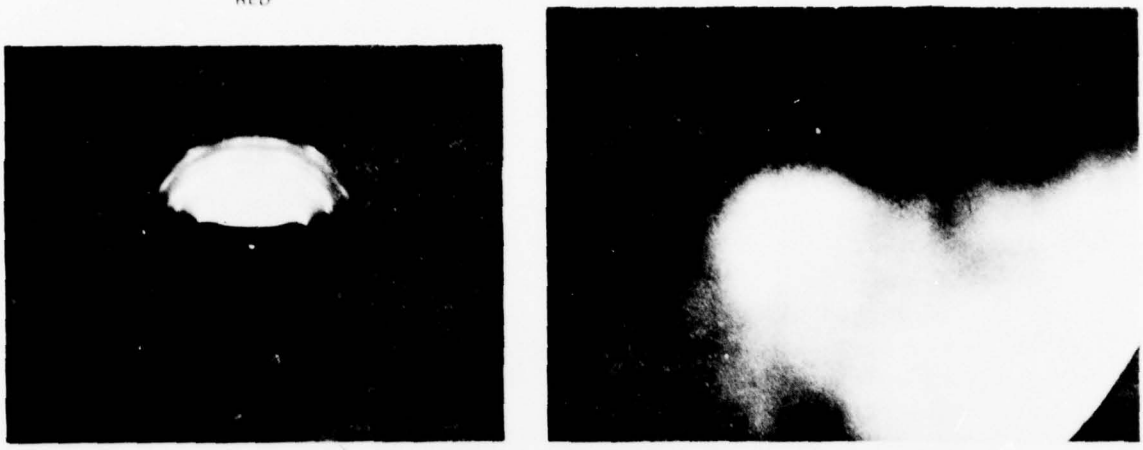

B. SINGLE CRYSTAL #8-18

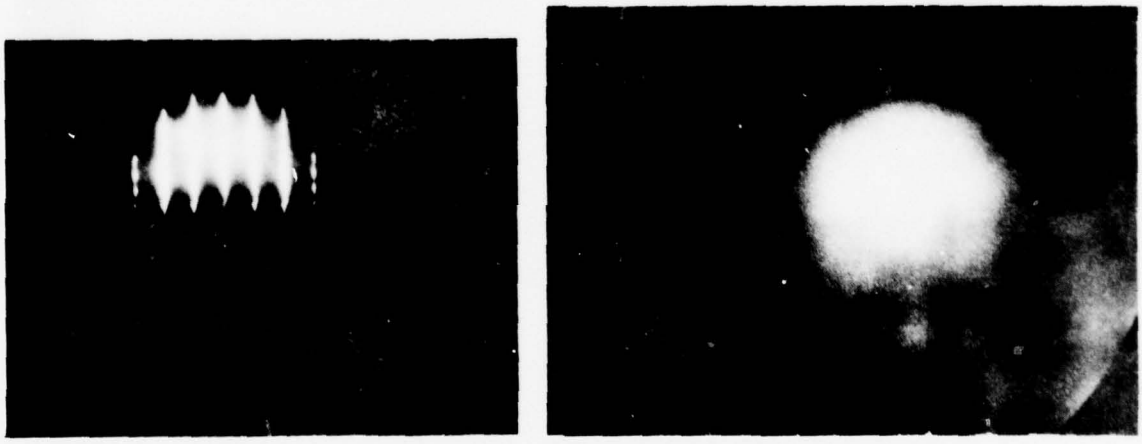

C. SINGLE CRYSTAL WITH KIKUCHI LINES #8-19

$$t = \frac{N \lambda_1 \lambda_2}{2 (\lambda_2 - \lambda_1) (n^2 - \sin^2\theta)^{1/2}}$$

where t is the film thickness, λ_1 and λ_2 are the wavelength at any two peaks or valleys in the spectrum, N is the number of peaks or valleys between λ_1 and λ_2, n is the index of refraction of the film, and θ is the angle of incidence of the beam.

The average index of refraction of the sputtered AlN films over the range of wavelengths from 350 millimicrons to 750 millimicrons was experimentally determined using one of the films grown in this program. Sample number 21 grown at a substrate temperature of 1257°C, target input power of 6.3 watts/cm^2 and background gas pressure of 2×10^{-2} torr was cut, mounted so that the two halves had their film surfaces in contact, and polished. From a calibrated photomicrograph, Fig. 5, and with a calibrated microscope reticle, the film thickness was measured and used to solve the interference equation above for n, the average index of refraction. The average index of refraction for the sputtered AlN along the c axis was found to be 2.37. However, because of the possibilities of strong dispersion of the index over the range of wavelengths used, the value of 2.37 for the index must be used with caution. In order to get an idea of the degree of dispersion in sputter AlN films, values of the index were calculated between every peak and valley of the interference spectrum generated by the spectrophotometer. This data is shown in Fig. 6 for wavelengths from 200 millimicrons up to 750 millimicrons. As a comparison with index values for bulk AlN, a pair of published (Ref. 10) AlN dispersion curves is also shown. Note that the index for the sputtered film begins to increase at much longer wavelengths than the bulk material does. This is probably due to the presence of a high level of strain in the films and to the presence of impurities entrapped in the film.

Data in the range from 350 millimicrons to 750 millimicrons was used to determine the coefficients in the expression:

$$n = A + \frac{B}{\lambda^2} + \frac{C}{\lambda^4}$$

by a least squares fit. This is the Cauchy equation which represents the normal dispersion curve in the visible region with good accuracy. From the least squares fit, the Cauchy equation for the index of refraction of sputter AlN in the 350 to 750 millimicron range was found to be

$$n = 2.17 + \frac{0.0157}{\lambda^2} + \frac{0.0052}{\lambda^4}$$

FIG. 5

POLISHED SECTION OF AlN FILM ON SAPPHIRE
SAMPLE #21

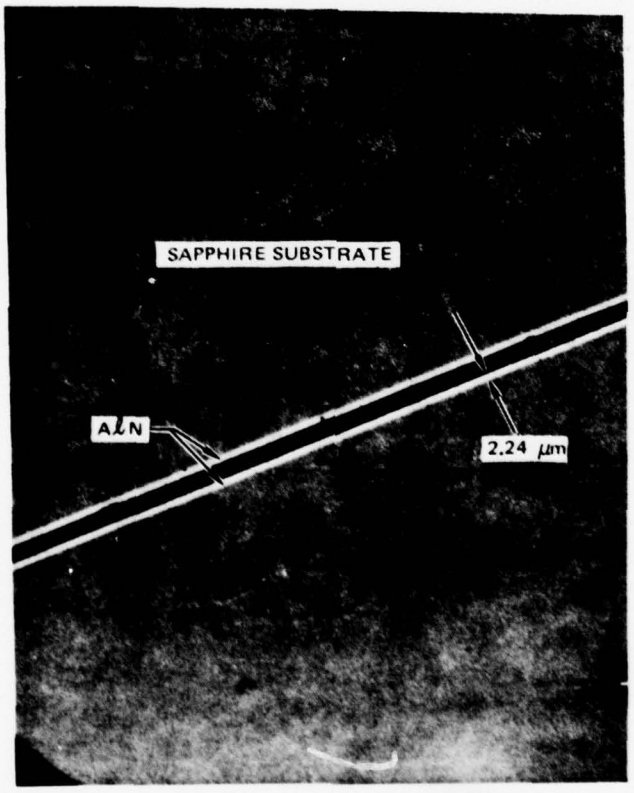

SPECTRAL DEPENDENCE OF THE REFRACTIVE INDEX OF SPUTTERED AIN COMPARED WITH BULK CRYSTAL VALUES OF AIN

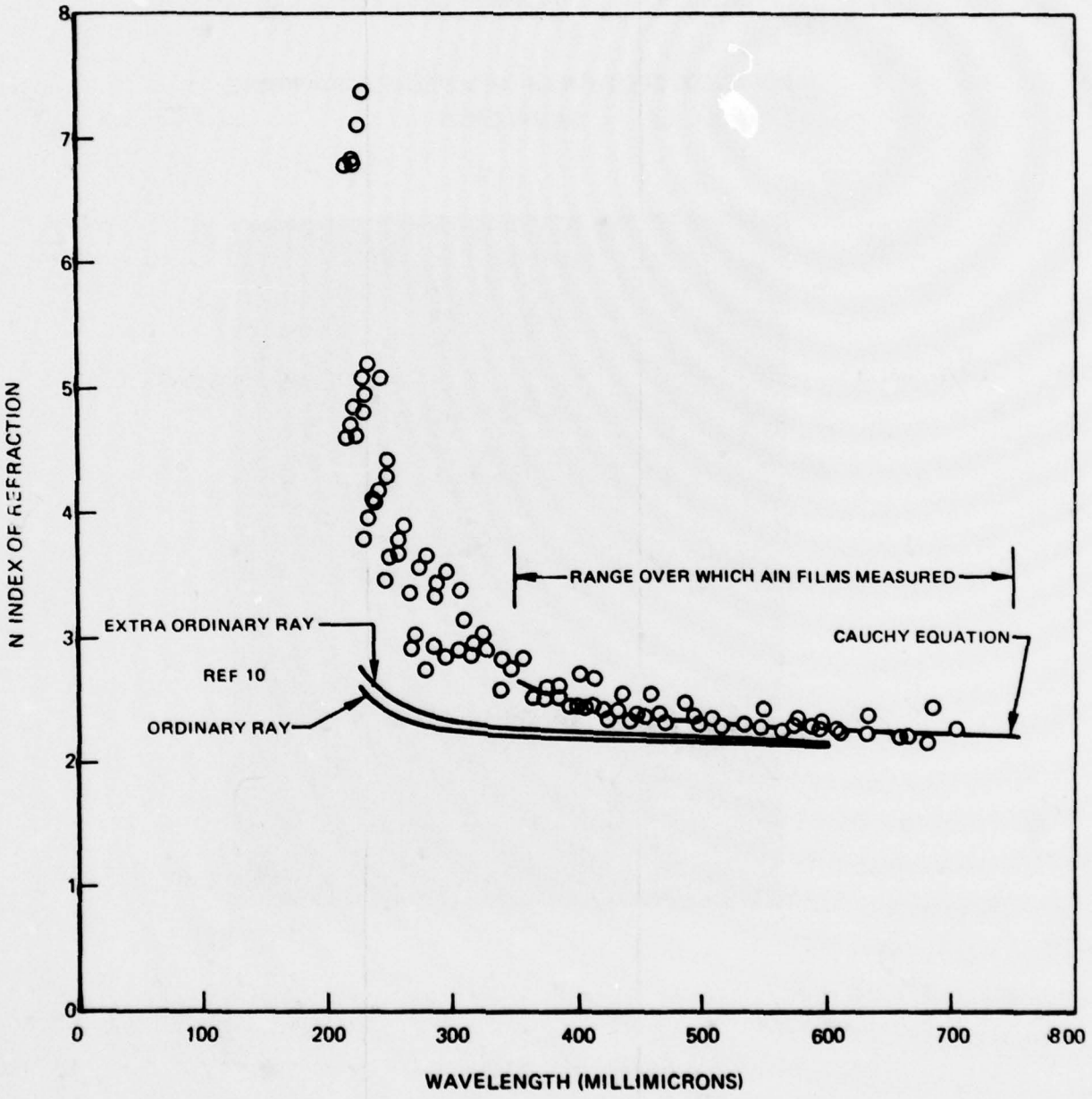

78-04-265-1

where λ is the wavelength of interest expressed in microns. From our previous work, Ref. 6, the index of sputtered AlN was measured to be 2.15 at a wavelength of 0.6328 μm. The earlier value was obtained by an analysis of guided optical modes in the sputtered film. At a wavelength of 0.6328 μm, the Cauchy equation predicts a value of 2.25 for the present work. The bulk values of the index at 0.6328 μm are seen to be 2.18 for the ordinary ray and 2.22 for the extraordinary ray.

To determine film thickness, the spectrophotometer was always operated over the range between 0.350 μm and 0.750 μm. The thickness of the film was calculated by using all of the peaks in the interference spectrum between these wavelengths. The average value of 2.37 for the index was used throughout. It is interesting to note that the mean value of the index as determined in the least squares fit of the Cauchy equation is also 2.37, in agreement with the average value found above. With the use of the spectrophotometer we verified that we were able to hold film thickness uniformity across the sample well within the 0.1 μm tolerance specified in the contract.

C. Aluminum Nitride Film Deposition on 25.4 x 9.0 x 2.0 mm (0001) Sapphire Substrates

1. Substrate Evaluation and Preparation

The substrates used for film deposition in this program were purchased from Insaco, Inc. The specifications provided to the vendor were that the substrates be:

- single crystal aluminum oxide.
- 25.4 ± 0.25 mm x 9.0 ± 0.25 mm x 2.0 ± 0.05 mm in size.
- (0001) ± 2° orientation.
- one side optically polished and free from scratches and gross defects under 80X magnification, opposite side to be ground to approximately 32 microinches.
- bowing of free standing substrate to be less than 2 wavelengths of sodium light over 80 percent of the polished face.

When the substrates were received, they were examined for flatness by observing the fringe patterns under an optical flat. The polished surface finish was examined under 100X magnification with a Leitz Orthoplan monocular microscope. Two substrates were returned because they did not meet the flatness

requirement. Each substrate was assigned a number at the time of its receipt so that each sample's history could be traced.

It was learned after the conclusion of the technical work portion of this program that microscopic examination of the substrates under conventional illumination was not sufficient to reveal the presence of shallow scratches in the substrates. Examination of the substrate using a stereo microscope with coaxial illumination revealed the presence of many scratches in the substrate even under low magnification. These scratches were also visible using an optical microscope with interference contrast illumination. Using a calibrated reticle in the microscope, it is estimated that the width of these scratches was 3 to 5 μm.

In order to get an estimate of the depth of these scratches, several sapphire substrate surfaces were measured with a profilometer. Figure 7 shows a portion of the surface profile of one substrate that appeared particularly bad under stereo microscopic examination. Note that the profile is generally quite smooth except for the presence of several shallow depressions. These depressions are about 200 Å deep and 5 μm wide. They are the only evidence found to testify to the presence of the scratches. The profilometer was calibrated immediately after the sapphire substrates were measured and found to be accurate within 1.5% of the calibration standard. The profilometer stylus radius of curvature is 2.5 μm. Therefore, while the substrates appeared to be unacceptable as viewed under special lighting, in reality the scratches are very shallow compared to the 2 μm thickness of the AlN film which was later deposited on them. Furthermore, since the sputtered films replicate the surface of the substrates faithfully, the presence of a scratch in the substrate does not represent a local thinning of the film but rather a small local waviness. In this case the waviness is estimated to be less than 1% of the film thickness.

Substrates were cleaned using the same sequence developed for the small substrates in the early part of the program (Sec. II-B1). Substrates were cleaned as needed just prior to loading into the chamber. Substrates were loaded into the chamber through the viewing port. The chamber was continuously purged with dry nitrogen during the loading sequence and pumped immediately after loading was completed. After the chamber had pumped out to about 5×10^{-7} torr, the heater was brought up to 1250°C and the system was allowed to pump overnight. Typically the chamber pressure had reached 6×10^{-8} torr prior to the start of deposition on the following day.

2. AlN Film Production

From the excellent results gained in the early part of the program with the small thin substrates, we felt that the operating parameters were pretty well established for growing AlN films. Accordingly, the deposition conditions

FIG. 7

TALYSURF TRACE OF POLISHED SIDE OF SAPPHIRE
SUBSTRATE #41

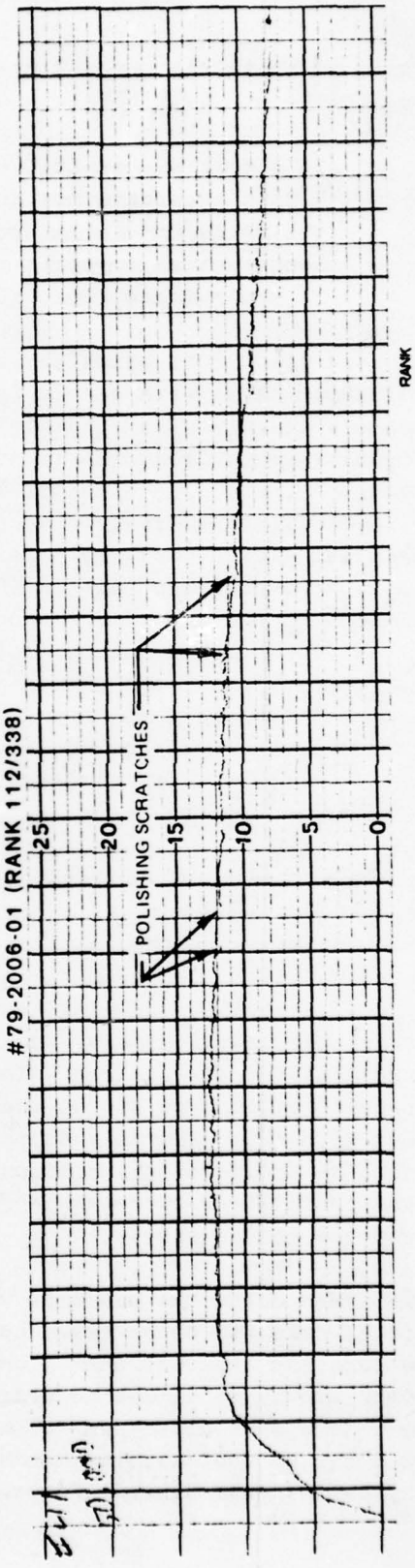

78-04-182-2

used were the same as those that we had previously determined to produce single crystal AlN vis

20 m torr NH_3 sputtering gas pressure
1250°C substrate heater temperature
6.3 watts/cm^2 target power density
longitudinal magnetic field
70 Å/min deposition rate.

Subsequent deposition runs using these deposition conditions produced erratic results. Some films were nearly free of inclusion while others were not. Those that had inclusion had them in varying amounts but all of the inclusions had one of three characteristic shapes. The shapes, as seen through an optical microscope, were 1) a straight line segment, 2) a Y shape, and 3) an X shape. Clearly, this type of pattern resulted from some form of crystalline dendritic growth. Figure 8 is a scanning electron microscope photograph of a typical growth on AlN on (0001) sapphire. Note that the angles between the branches of the growth are about 60° and 120°. These angles are expected for crystalline growth on the (0001) plane. An electron microprobe analysis of the composition of the growths revealed that the only difference between their composition and that of the smooth part of the film was that they contained silicon. Because silicon and silicon dioxide both have vapor pressures of about 10^{-5} torr at 1250°C, there was a distinct possibility that silicon was being evolved from some component of the substrate heater.

As previously stated, the substrate heaters used in this process are aluminum oxide coated molybdenum strip heaters. As a precaution, to prevent the heater from contaminating the substrate, a "high purity" 0.8 mm thick aluminum oxide slide was placed over the heater to act as a shield between the heater and the substrate. Several samples of Al_2O_3 slides used in the system for various amounts of time as well as one slide which had not been used at all were analyzed for silicon. The electron microprobe analysis revealed no trace of silicon on any of these samples. However, by replacing the Al_2O_3 slides with a 0.5 mm thick sapphire wafer, the dendritic growth was eliminated. The origin of the silicon is still unexplained although it is possible that the silicon is released from the interior of the ceramic where the microprobe cannot sample.

Films were grown using the sapphire wafer liners for the remainder of the program. However, care had to be taken during start up not to thermally shock the sapphire wafers and fracture them. During shutdown, it was also required to decrease power slowly so as not to crack the AlN film as well as the sapphire liners. Figure 9 is a photomicrograph of an AlN film on a sapphire substrate which had crazed due to too rapid a shutdown sequence. Note that the fractures occur along crystalographic lines. Figure 10 is a high magnification electron

FIG. 8

SEM PHOTOGRAPH OF DENDRITIC GROWTH ON AIN ON (0001) SAPPHIRE #11-2

FIG. 9

CRAZED AlN FILM ON (0001) SAPPHIRE SAMPLE NO. 12

78-04-255-1

FIG. 10

ELECTRON MICROSCOPE VIEW OF CRAZED AlN FILM SAMPLE NO. 12

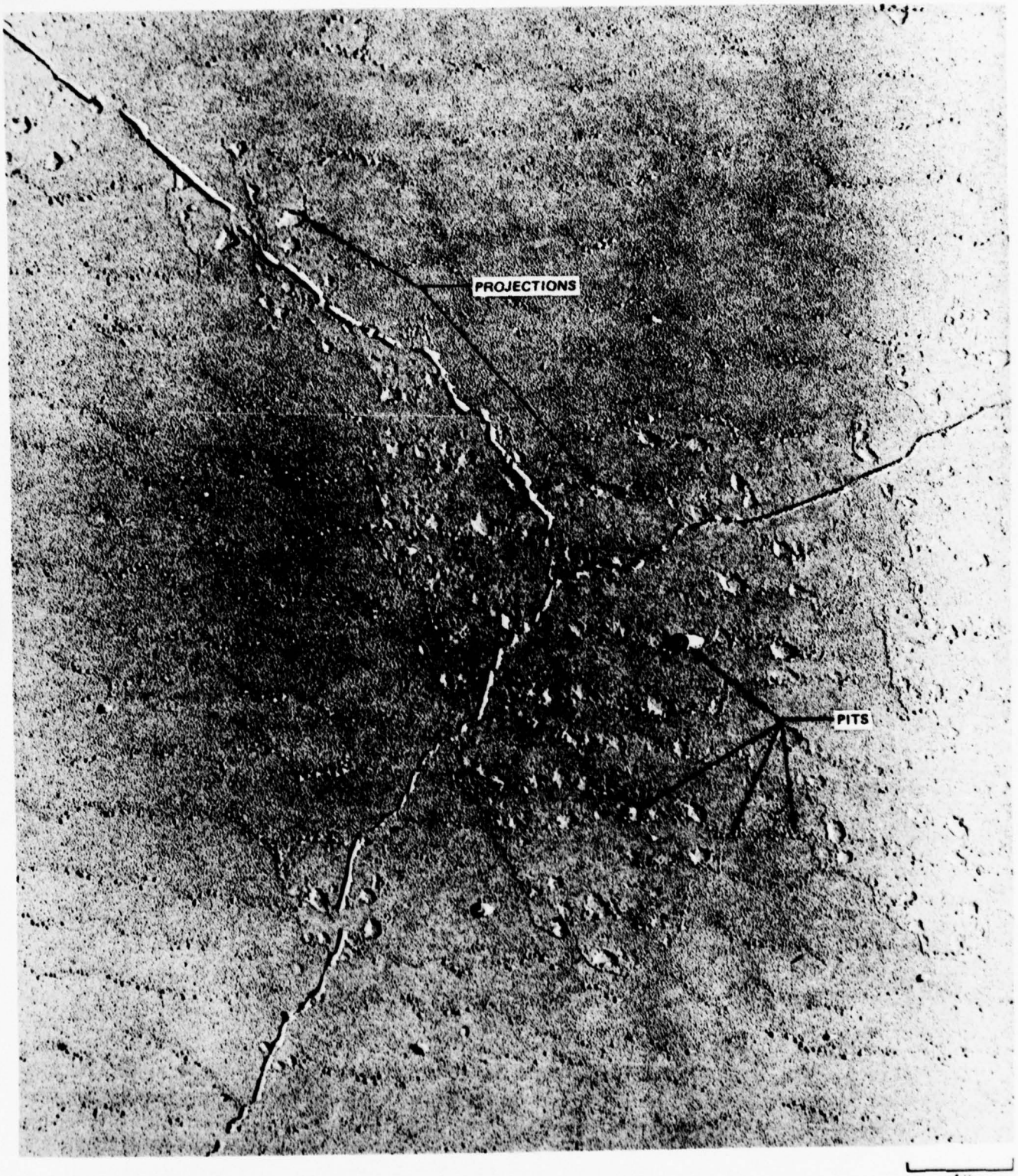

78-04-255-2

microscope view of the same AlN film as shown in Fig. 9. This view was taken using replication and shadowing techniques. The shadowing was done with a source at approximately 30° up from the plane of the film. From this view, we see that the cracks in the film have not opened indicating that the crazing took place with the film under compression. From this view we can also see the presence of many small pits in the film which are of the order of 0.01 μm in diameter and 0.04 μm deep. A few larger pits up to 0.16 μm diameter and 0.13 m deep are also evident. There are also a number of nondescript projections which appear to be clustered in the vicinity of the cracks. These projections may have been present on the substrate.

As the program progressed it was noted that the deposition rate was decreasing slowly. The decrease occurred in spite of seemingly constant deposition conditions. It was noted at this time that the crystalline quality of the film, as indicated by electron channeling analysis, was also deteriorating. The power density to the target was subsequently increased to 7.1 watts/cm^2, to bring the deposition rate back up. The crystalline quality of the film also improved as a result of increasing the deposition rate. Attempts to pursue this trend by increasing the power density further resulted in producing grainy films. Accordingly, the power density to the target was maintained at 7.1 watts/cm^2 for the remainder of the program. A total of 37 samples were produced in this program. Figure 11 is a high magnification view of a grainy film. From an analysis of the shadows cast in this view, the depth of the crevices are of the order of 0.2 μm.

3. AlN Film Evaluation

Films were examined immediately after removing them from the growth station. The examination was made at 100X, 200X, and 500X magnification with a Leitz Orthoplan microscope. Films were completely scanned and the quality of the films was assessed as to texture, clarity, and presence of occlusions and pits. The criteria which was not met most often was that of optical surface quality. Yet the aspect of the process to which we gave our greatest attention was precisely that of achieving clear, fault-free films. The predeposition cleaning process of the substrates is the most painstaking one in the entire coating sequence. However, the possibility of contamination occurring during loading and during deposition is still considerable for surfaces as large as those presented by the 25.4 x 9.0 mm substrates.

The thickness of the film was measured at three locations across the substrate. The measurements were made at the center of the film and approximately 2 mm from each end. The method used was through interference spectroscopy as previously described in Sec. II-B3. Figure 12 is a reproduction of a typical set of interference curves taken during this program. It is estimated that the maximum error introduced due to estimating the position of the interference peaks and valleys is ± 0.015 μm in film thickness.

FIG. 11

ELECTRON MICROSCOPE VIEW OF GRAINY AlN FILM SAMPLE NO. 45

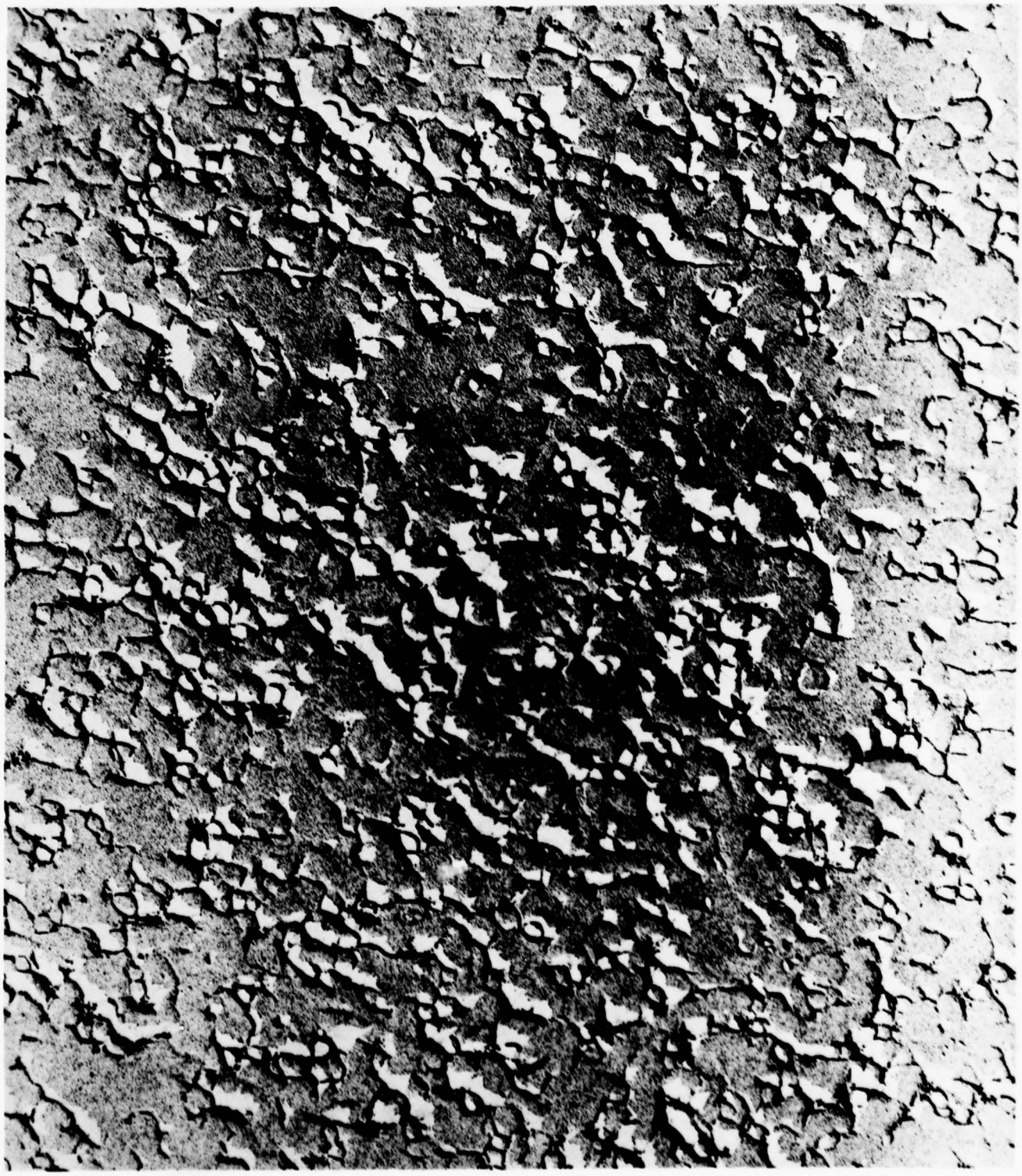

1 μ

78-04-255-3

FIG. 12

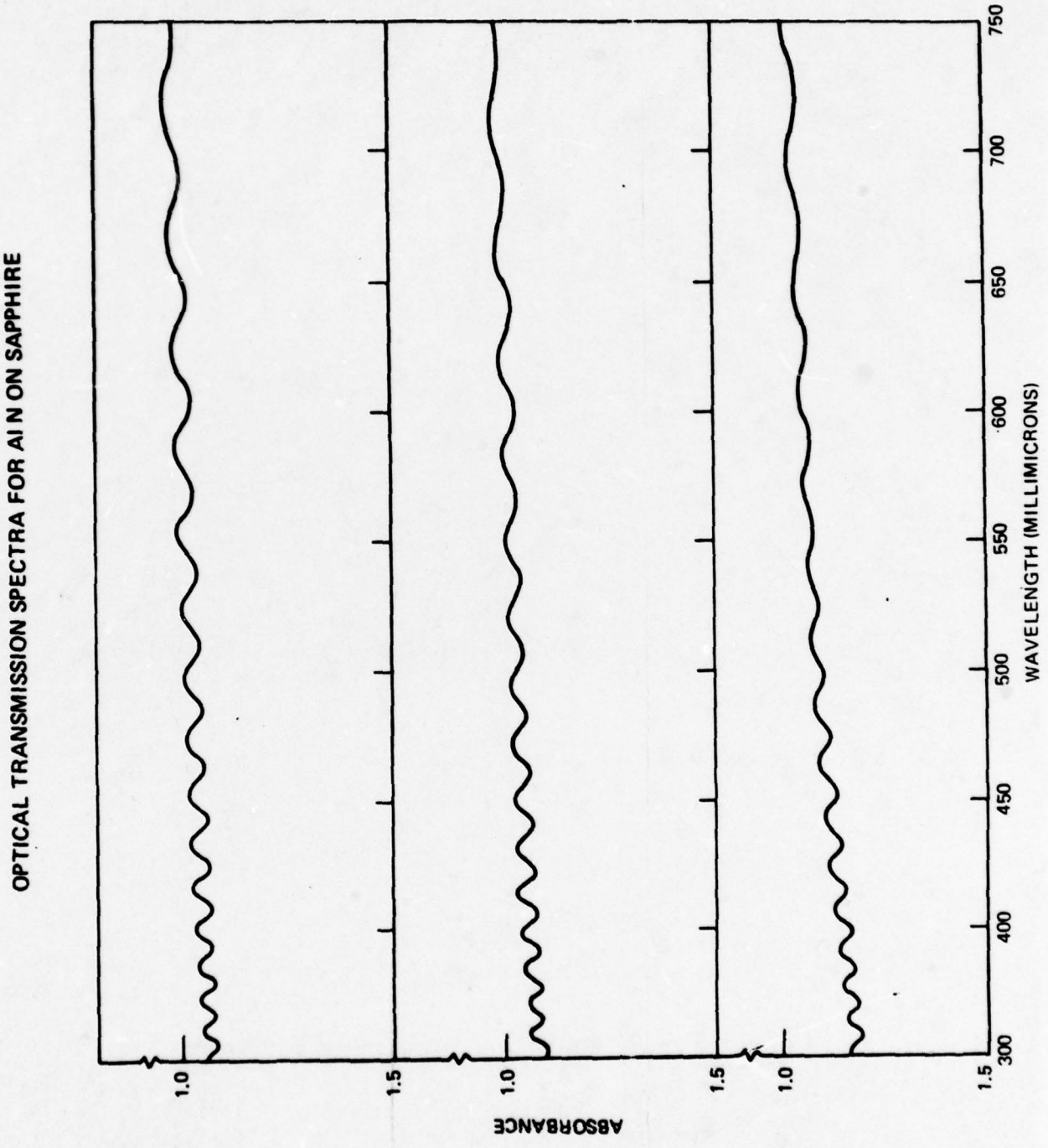

77-09-218-2

The film thicknesses of the twelve samples delivered for this program are listed in the table below:

Sample Number	AlN Film Thickness - Microns
9	2.28 ± 0.02
10	$2.00 \begin{smallmatrix} +0.02 \\ -0.03 \end{smallmatrix}$
14	$2.19 \begin{smallmatrix} +0.06 \\ -0.03 \end{smallmatrix}$
20	2.28 ± 0.01
25	$2.30 \begin{smallmatrix} +0.03 \\ -0.05 \end{smallmatrix}$
29	$2.12 \begin{smallmatrix} +0.03 \\ -0.01 \end{smallmatrix}$
31	2.23 ± 0.01
33	2.08 ± 0.02
36	$2.13 \begin{smallmatrix} +0.02 \\ -0.03 \end{smallmatrix}$
50	2.09 ± 0.01
51	$2.15 \begin{smallmatrix} +0.04 \\ -0.01 \end{smallmatrix}$
52	$2.17 \begin{smallmatrix} +0.02 \\ -0.01 \end{smallmatrix}$

The film structure was evaluated using electron channeling and x-ray analysis. The electron channeling method of film analysis was chosen because of the ease with which the complete area of the AlN film could be analyzed and because of the relatively large samples which could be accommodated in the instrument. As mentioned previously in Section II-B3, a comparison was made between the type of pattern seen under RED and under electron channeling for single crystal AlN. However, as pointed out in Section II-B3, electron channeling is a very critical test for single crystal structure since the pattern formed depends on similar mechanisms as does the formation of Kikuchi lines. The electron channeling patterns obtained from the AlN on the 25.4 x 9.0 x 2 mm substrates were not as sharp as that shown in Fig. 4C but rather more of the type shown in Fig. 4B. Figure 13 is a typical electron channeling pattern for AlN on a 25.4 x 9.0 x 2.0 mm substrate. A factor which contributed to the loss of resolution in the electron channeling analysis was that a thin layer of amorphous carbon had to be applied to the AlN film to make it elec-

FIG. 13

ELECTRON CHANNELING PATTERN OF AIN ON 25.4x9x2mm (0001) SAPPHIRE SUBSTRATE #29

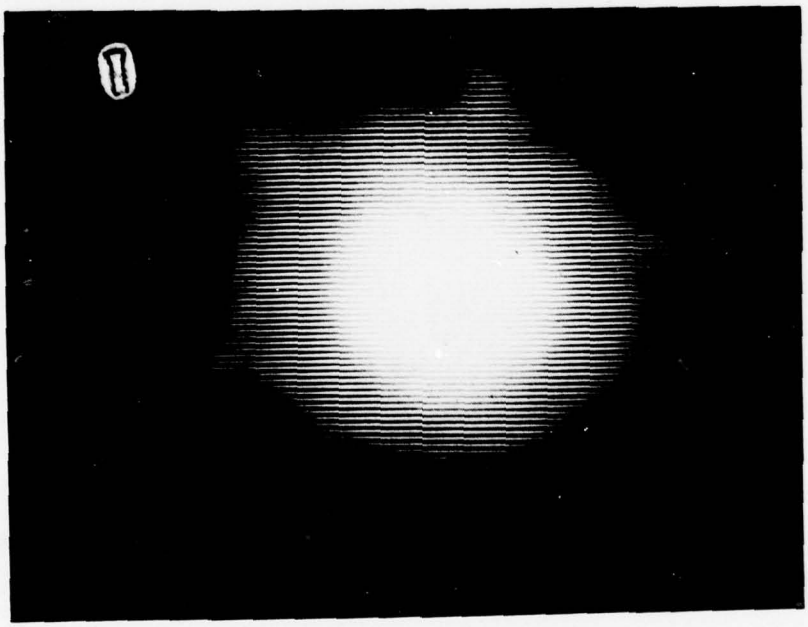

trically conductive. This was necessary to keep the sample from charging in the electron beam and thereby distorting the channeling pattern.

All AlN films were examined with electron channeling. In all cases, the sample was scanned over its entire area. In no instance was the pattern found to vary. This indicated that the film was of uniform crystal quality over the entire area of the substrate.

In addition to the electron channeling pattern, x-ray diffractometer scans were also taken of the deliverable AlN samples. Figure 14 shows a typical scan for the AlN film on (0001) sapphire substrate produced in this program. Note that the major peaks in the scan all indicate that the AlN film is oriented with its basal plane parallel to the basal plane of the sapphire substrate. The position of the (0002) AlN peak relative to the position of the (0006) Al_2O_3 peak implies a lattice spacing of the basal planes of 4.99 Å for AlN. This value compares very favorably with the reported values listed below.

Investigators	AlN Lattice Constant "C" (Å)
Ott[11]	4.981
Stackelberg and Spiess[12]	4.96
Jeffrey and Parry[13]	4.980
Kohn, Cotter, and Potter[14]	4.965
Paretzkin[15]	4.986
Taylol and Lenie[16]	4.980
Yim and Paff[17]	4.980

The smaller peaks seen at about 40° and below 36° appear to be due to an ammonia molybdenum nitrate compound impurity in the film. It is not surprising to find such an impurity in view of the fact that we deposited these films in an ammonia atmosphere using a molybdenum heater. The presence of gas entrapment in sputtered films has been reported by others (Ref. 18). One method of reducing gas entrapment is to sputter at higher rates or reduced gas pressure. The problem of molybdenum contamination might be solved by replacing the heater with an rf induction heated graphite susceptor.

None of the low level background peaks appear to be associated with other crystallographic planes of AlN. This says that although there are some impurities, maybe of the order of a few percent, in the AlN film, this has not in-

R78–922937–4

FIG. 14

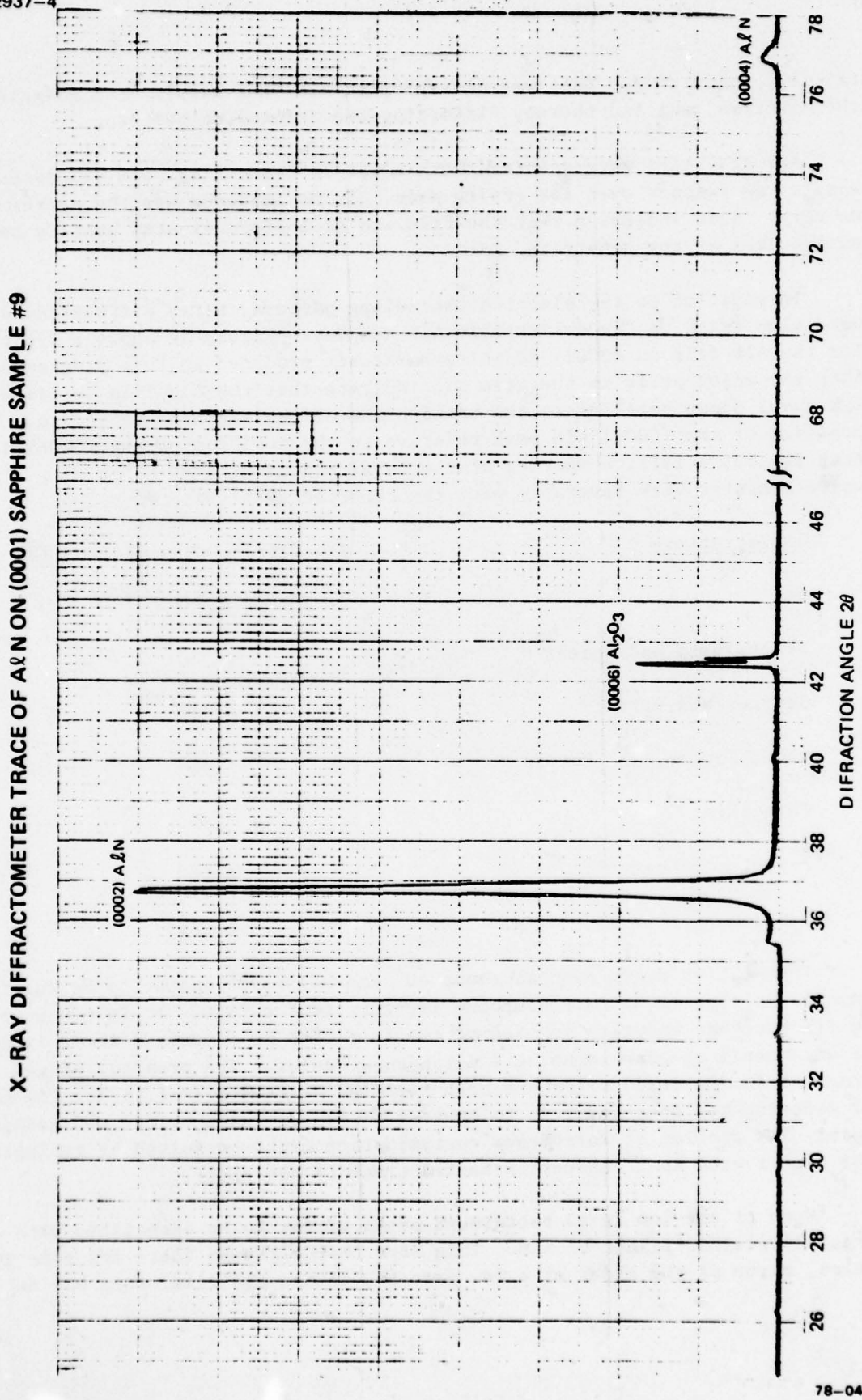

terfered with the film's overally crystalographic orientation and furthermore that the AlN film has grown with its [0001] direction normal to the substrate surface. All of the AlN films analyzed with x-ray diffraction showed the same pattern of low level background impurity peaks. Sample 8-19, Fig. 4C, whose RED and electron channeling patterns were some of the best we have ever seen for rf sputtered films, also exhibited the same low level background peaks under x-ray diffractometer ana sis.

D. Measurement of Acoustoelectric Properties

The measurement of piezoelectric and acoustic properties for sputtered AlN on sapphire samples was carried out on selected samples by fabricating surface acoustic wave (SAW) transducers and delay line structures on the AlN film surface (Refs. 7, 19). Figure 15 shows a schematic view of two interdigital electrode transducers which are fabricated on a rectangular substrate to form a single delay line with acoustic propagation aligned along the substrate long dimension. Transducers of this type are fabricated by photolithography (Ref. 20) using an aluminum thin-film with thickness near 1500 Å. During this program we fabricated transducers and delay lines on the 25.4 x 9.0 x 2.0 mm substrates in two basic configurations:

1) A series of identical transducers was fabricated on the substrate surface with propagation vector aligned along the 25.4 mm dimension, and
2) A series of identical transducer-pairs was fabricated with propagation vector aligned along the 9.0 mm dimension.

Although the propagation vector for these two configurations is different by 90°, the resulting acoustic device data is expected to be essentially equivalent for the two because of the low anisotrophy for the AlN on C-plane sapphire crystal structure. The first configuration was utilized during the early part of the program so that existing UTRC photomasks could be utilized. In addition, this configuration allows an accurate assessment of SAW propagation loss. The second confiuguration was used to simulate the multi-parallel acoustic delay path configuration used earlier by RADC on high frequency SAW filter bank devices (Ref. 21).

The acoustoelectric properties of AlN on sapphire were estimated by making a comparison of theoretical and experimental parameters associated with the operation of interdigital electrode SAW transducers and delay lines. Previous work (Refs. 19, 22) has shown that the input impedance of a SAW transducer can be modeled by a series equivalent circuit,

FIG. 15

SCHEMATIC VIEW OF A SURFACE ACOUSTIC WAVE DELAY LINE UTILIZING INTERDIGITAL ELECTRODE TRANSDUCERS

78-05-154-4

$$Z_{in} = R_c + j\omega L_c + R_a(f) + jX_a(f) + \frac{1}{j\omega C_T}. \quad (1)$$

where R_c and L_c are contact resistance and inductance parameters, $R_a + jX_a$ is a piezoelectrically excited radiation impedance; and $1/j\omega C_T$ is the capacitive reactance associated with the transducer interdigital electrode structure. The radiation reactance, X_a, is usually small compared to $1/\omega C_T$ and may therefore be neglected. The predominant frequency characteristics of this type of transducer are determined by the radiation resistance, R_a, which has the form (Ref. 23),

$$R_a(f) = \hat{R}_a \left[\frac{\sin N_g (\pi/2) (f/f_o - 1)}{N_g \sin (\pi/2) (f/f_o - 1)} \right]^2 \quad (2)$$

where

f_o = transducer wave synchronism frequency

$\hat{R}_a$ = peak value of radiation resistance

N_g = number of active acoustoelectric excitation gaps.

The peak radiation resistance is, in turn, related to the piezoelectric coupling constant (k^2) by

$$\hat{R}_a = \frac{2}{\pi} k^2 N_g (1/\omega_o C_T) \quad (3)$$

and the remaining parameters are

$\omega_o = 2\pi f_o$

$C_T = w N_g C_g$ = total transducer capacitance

w = transducer acoustic aperature

C_g = capacitance per gap unit length.

We note from the above that a measurement of radiation resistance versus frequency should yield a sin x/x type of response which peaks at $f = f_o$ and nulls at $|f/f_o - 1| = 1/2\ N_g$. Figure 16 shows an experimental measurement of <u>total</u> transducer resistance, $R_c + R_a$, versus frequency for one transducer of an AlN/sapphire delay line called M-521. Note that the background contact resistance, R_c, is almost constant over the 450 to 500 MHz frequency band and that the sin x/x behavior of R_a is clearly visible. Experimental plots like the one shown in Fig. 16 allow the determination of R_c, R_a, and f_o. Other, low frequency (1 MHz), measurements are used to determine C_T, and the gap parameter, N_g, is known from the transducer design. Thus, enough information is available to experimentally estimate k^2 from Eq. (3). Data obtained from AlN/sapphire transducers fabricated during this program gave $k^2 \sim 0.1\%$.

The data used to estimate k^2 can also yield estimates of other basic parameters. For example, it is known that the transducer and gap capacitance are proportional to the effective permittivity and dielectric constant seen by the transducer structure at the AlN/sapphire surface. Thus,

$$C_g = C_T/(w\ Ng) \sim \varepsilon', \tag{4}$$

which means that the effective dielectric constant for an AlN/sapphire sample may be estimated by comparison with data from another transducer-substrate configuration where ε' is known. The AlN/sapphire dielectric constant can then be estimated by proportion,

$$\varepsilon'_B = \varepsilon'_A\ C_{gB}/C_{gA} \tag{5}$$

Data obtained during this program with equivalent crystalline quartz devices ($\varepsilon' = 4.43$) gave $\varepsilon' = 8.3$ for 2 μm AlN films on C-plane sapphire.

The velocity of SAW propagation may also be estimated noting that,(Ref. 19)

$$f_o = v\ \lambda_o \tag{6}$$

where v is the desired velocity and λ_o is the periodic dimension of the interdigital electrode transducer. Data achieved during this program yielded $v \sim 5730$ m/s on C-plane sapphire.

FIG. 16

EXPERIMENTALLY MEASURED TRANSDUCER INPUT RESISTANCE VERSUS FREQUENCY
FOR PORT 2 OF AlN/SAPPHIRE DELAY LINE M-521

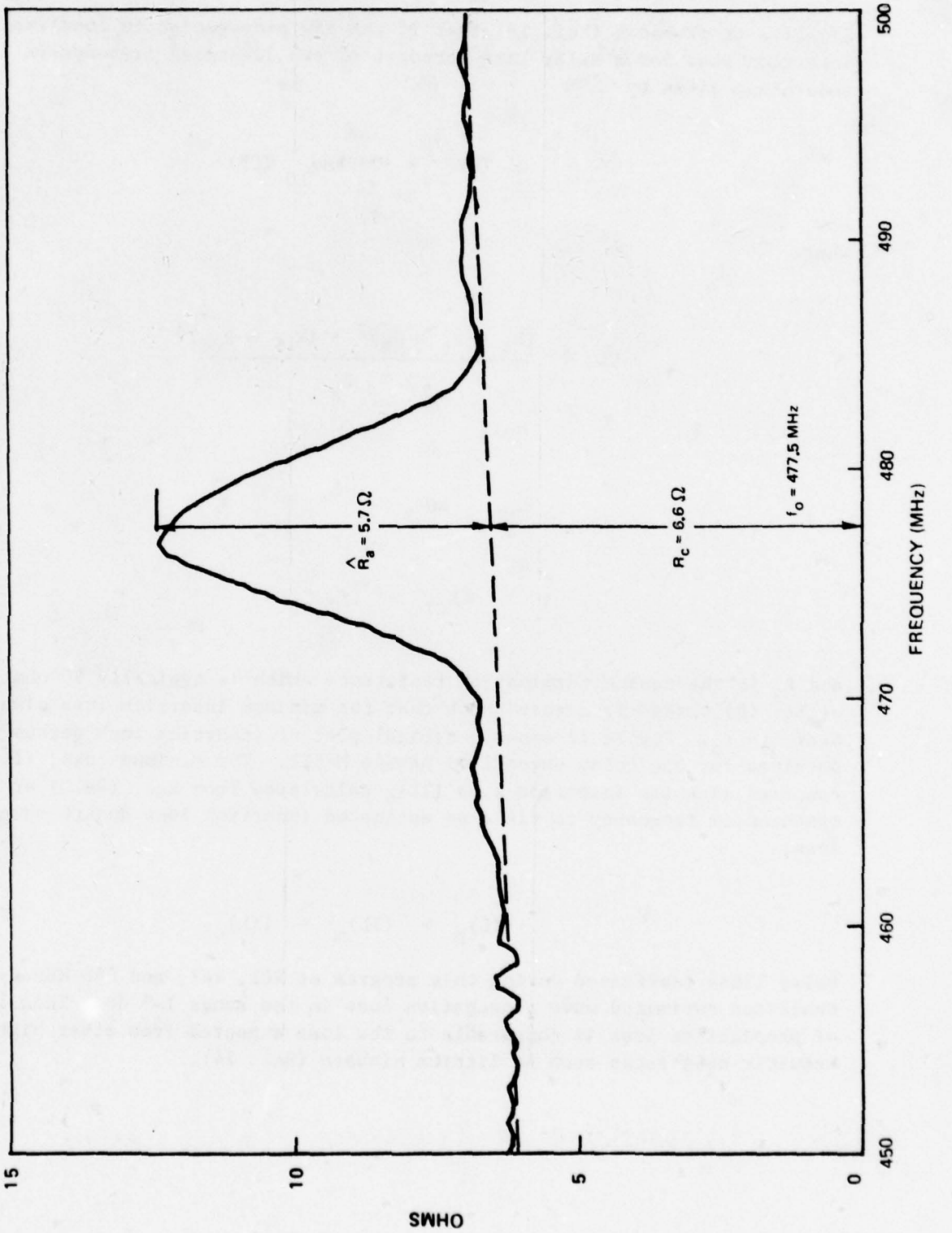

78-05-154-2

Finally, it is known (Ref. 19) that if the SAW propagation is lossless, the insertion loss for a delay line composed of two identical transducers is accurately given by

$$IL\ (dB) = 20 \log_{10} (CL) \tag{7}$$

where

$$CL = \frac{(R_a + R_c + R_g)^2 + (X_{LC} + X_{CT})^2}{2\ R_a\ R_g} \tag{8}$$

$$X_{LC} = \omega\ L_c \tag{9}$$

$$X_{CT} = 1/\omega\ C_T \tag{10}$$

and R_g is the source termination resistance which is typically 50 ohms. Analysis of Eq. (8) versus frequency shows that the minimum insertion loss always occurs near $f \sim f_o$. Figure 17 shows a typical plot of insertion loss versus frequency obtained for one delay channel of device M-521. The minimum loss, (IL)m, can be compared with the insertion loss $(IL)_o$ calculated from Eqs. (7-10) at the synchronism frequency to yield an estimated insertion loss due to wave propagation loss,

$$(IL)_p \simeq (IL)_m - (IL)_o. \tag{11}$$

Delay lines fabricated during this program at 201, 447, and 848 MHz typically exhibited estimated wave propagation loss in the range 1-3 dB. This low value of propagation loss is comparable to the loss expected from other high quality acoustic substrates such as lithium niobate (Ref. 24).

FIG. 17

EXPERIMENTALLY MEASURED DELAY LINE (TWO TRANSDUCER) INSERTION LOSS VERSUS FREQUENCY FOR CHANNEL 3 OF AlN/SAPPHIRE DELAY LINE M-521

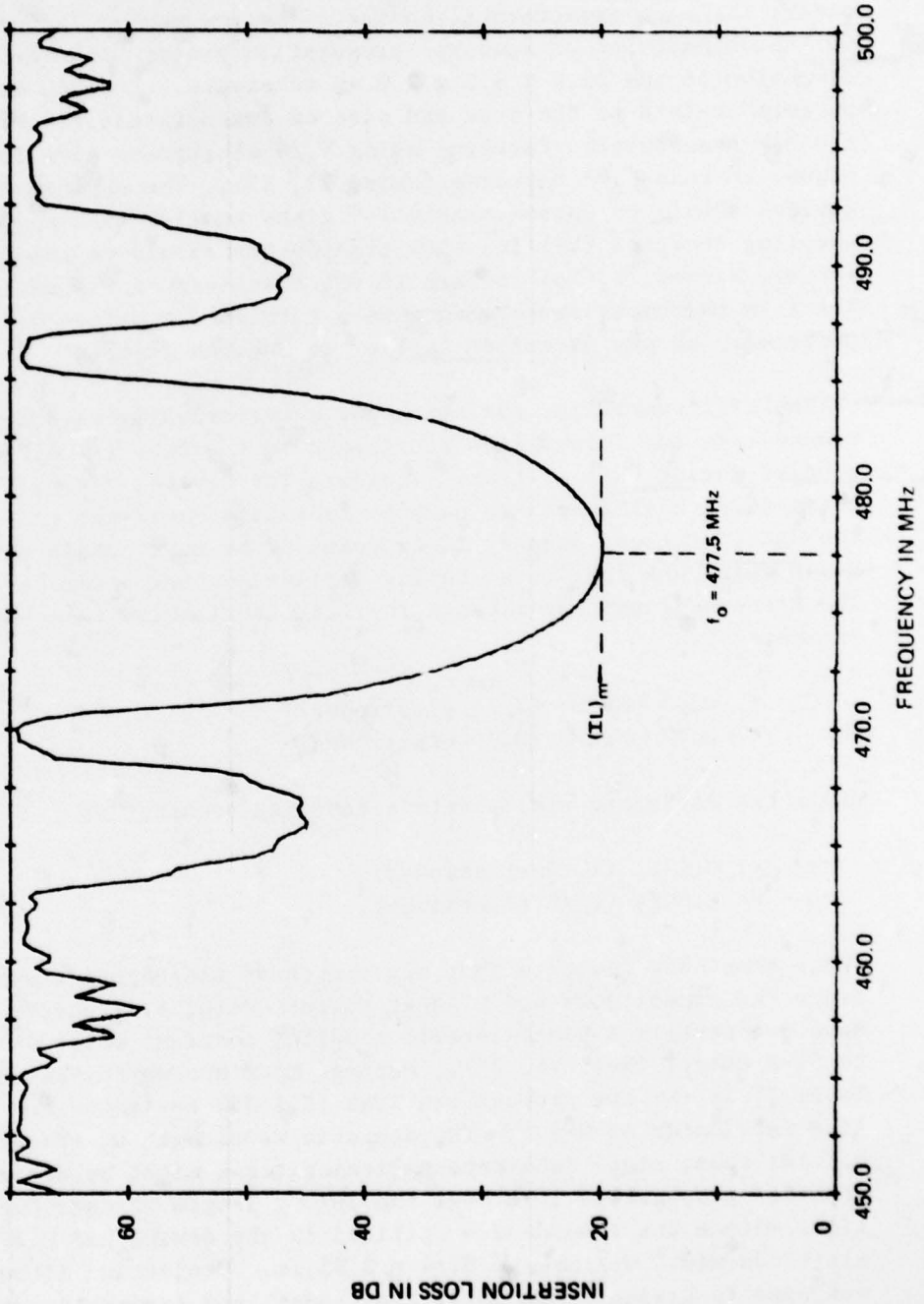

78-05-154-1

Four (4) AlN/sapphire transducer-delay lines were fabricated for operation at 201, 477, and 848 MHz. Table I provides a summary of the physical parameters for each experimental device. The row marked "acoustic conf." refers to the orientation of acoustic propagation vector with respect to the long dimension of the 25.4 x 9.0 x 2.0 mm substrate. The row marked "electrode pattern" refers to the type and size of interdigital electrode pattern used in the SAW transducer. Patterns using $\lambda_o/4$ electrodes have lower capacitance and higher k^2 than $\lambda_o/8$ patterns (Refs. 22, 25). The capacitance for $\lambda_o/4$ electrode devices should be approximately 1.4 times smaller than $\lambda_o/8$ designs while the coupling constant (k^2) for $\lambda_o/4$ transducers should be about 1.4 times higher. The row marked "$t_f(\mu m)$" refers to the thickness of AlN measured for each device. The film thickness measurements were carried out using intereference spectrophotometry as was described earlier in Section II-B3.

Table II summarizes the important experimentally measured parameters for transducers and delay lines fabricated on the four (4) AlN/sapphire samples studied during this program. The data for devices M-485, M-521, and M-533 was obtained with AlN/sapphire samples fabricated near the end of this program; thus, the data for these samples is expected to be more consistent than data for M-440 which was fabricated during earlier sputter parameter adjustment studies. The transducer gap capacitance in later fabrication runs appears to be well estimated by

$$C_g = 0.05 \text{ pF/mm} \quad (\lambda_o/4 \text{ electrodes})$$
$$= 0.07 \text{ pF/mm} \quad (\lambda_o/8 \text{ electrodes})$$

while the estimated piezoelectric coupling constant is

$$k^2 = 0.12\% \quad (\lambda_o/4 \text{ electrodes})$$
$$= 0.09\% \quad (\lambda_o/8 \text{ electrodes})$$

These constants indicate that our sputtered AlN/sapphire samples have approximately twice the capacitance and ϵ' that corresponding ST-X quartz substrates would have but possess a piezoelectric coupling constant which is almost identical to ST-X quartz (Ref. 24, 26). Perhaps most noteworthy in the data shown in Table II is the low propagation loss (2.1 dB) estimated for the 848 MHz delay line fabricated on M-533. The acoustic wavelength at this frequency is only 6.8 μm; thus, small substrate polishing flaws might be expected to yield substantial propagation loss over the 307 λ_o length of this two transducer delay line. Since the transducers utilized in the device had $\lambda_o/8$ electrodes, the electrode width was tobe 6.81/4 = 0.85 μm. Projection lithography (Ref. 26) was used to create these small electrodes, and Figure 18 shows a SEM photo of the electrodes in one transducer of M-533. Note the excellent edge acuity

TABLE I

PHYSICAL PARAMETERS FOR AlN/SAPPHIRE
TRANSDUCER-DELAY LINES

Parameter	M-440	M-482	M-521	M-533
f_o (MHz)	201.2	475.0	477.5	848.3
λ_o (μm)	28.44	12.00	12.00	6.81
N_g	221	119	119	239
w (mm)	1.0	1.0	1.0	0.26
electrode pattern	$\lambda_o/8$	$\lambda_o/4$	$\lambda_o/4$	$\lambda_o/8$
acoustic conf.	parallel	perp.	perp.	parallel
t_f (μm)	2.34	2.22	2.13	1.94

TABLE II

EXPERIMENTAL PARAMETERS ESTIMATED FOR
AlN/SAPPHIRE TRANSDUCER-DELAY LINES

Parameter	M-440	M-482	M-521	M-533
f_o (MHz)	201.2	475.0	477.5	848.3
v (m/S)	5722	5700	5734	5777
C_T (pF)	13.6	5.5	6.0	4.6
C_g (pF/m)	0.062	0.046	0.05	0.074
ϵ'	7.5	7.8	8.3	8.6
$\hat{R}_a$ (ohms)	4.7	5.6	5.8	5.5
k^2 (%)	0.057	0.12	0.14	0.089
R_c (ohms)	5.0	6.0	6.5	13
L_c (nH)	14	16	13	11
(IL) m	21.3 dB	20.2 dB	20.0 dB	21.4 dB
(IL) o	20.8 dB	17.1 dB	17.2 dB	19.3 dB
(IL) p	0.5 dB	3.1 dB	2.8 dB	2.1 dB

FIG. 18

SCANNING ELECTRON MICROSCOPE PHOTOGRAPH OF AN INTERDIGITAL ELECTRODE TRANSDUCER USED IN M-533

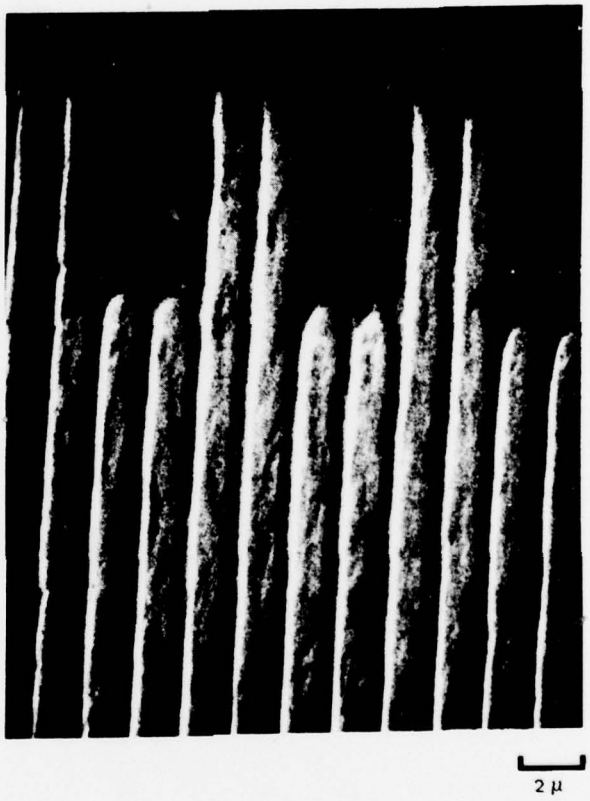

78-05-166-1

of these small electrodes and the relative smoothness of the AlN/sapphire surface. Analysis of the SEM photograph shows that the electrode widths are approximately 1.1 μm wide and the gap widths are about 0.4 μm wide. Recent experimentation with exposure time in the photolithographic process has resulted in more nearly equal electrode and gap widths. The quality of photolithography and sample surface smoothness of M-533 led to excellent high frequency delay line characteristics as can be seen from the plot of delay line insertion loss versus frequency shown in Fig. 19. The smooth sidelobe response indicates that electromagnetic feedthrough signals are attenuated by at least 70 dB; high values of feedthrough attenuation are desirable for parallel filter bank operation (Ref. 21).

A final key point which was gained from analysis of data on AlN/sapphire delay lines constructed near the end of this program was that the delay lines fabricated at several physical locations on the 25.4 x 9.0 mm substrate surface exhibited exceptionally uniform data. For example, device M-521 had six (6) delay channels (two transducer pairs in each channel) aligned parallel to the 9.0 mm dimension and spaced by 4.0 mm uniformly over the 25.4 mm substrate dimension. Due to I/O connector limitations, only three (3) channels were actually wire bonded and measured. Channels 1 and 3 were located at the extreme ends of the 25.4 mm substrate length and channel 2 was located at one of the two central positions. Since each delay channel had two transducers and the pattern for all transducers was identical, it was possible to record data from six (6) widely separated transducer locations which could be assessed for transducer parameter (and AlN/sapphire) uniformity. Data was recorded for the low frequency (1 MHz) capacitance at each measurement port (i.e., at each transducer):

Port	Capacitance (pF)
1	5.80
1'	6.46
2	5.73
2'	5.73
3	6.24
3'	5.82
	5.96 ± 0.31 pF

This data indicated that it was physically possible to fabricate six (6) transducers at widely different substrate locations with relatively good electrode capacitance uniformity.

FIG. 19

EXPERIMENTALLY MEASURED DELAY LINE INSERTION LOSS VERSUS FREQUENCY
FOR THE 850 MHz AlN/SAPPHIRE DELAY LINE (M-533)

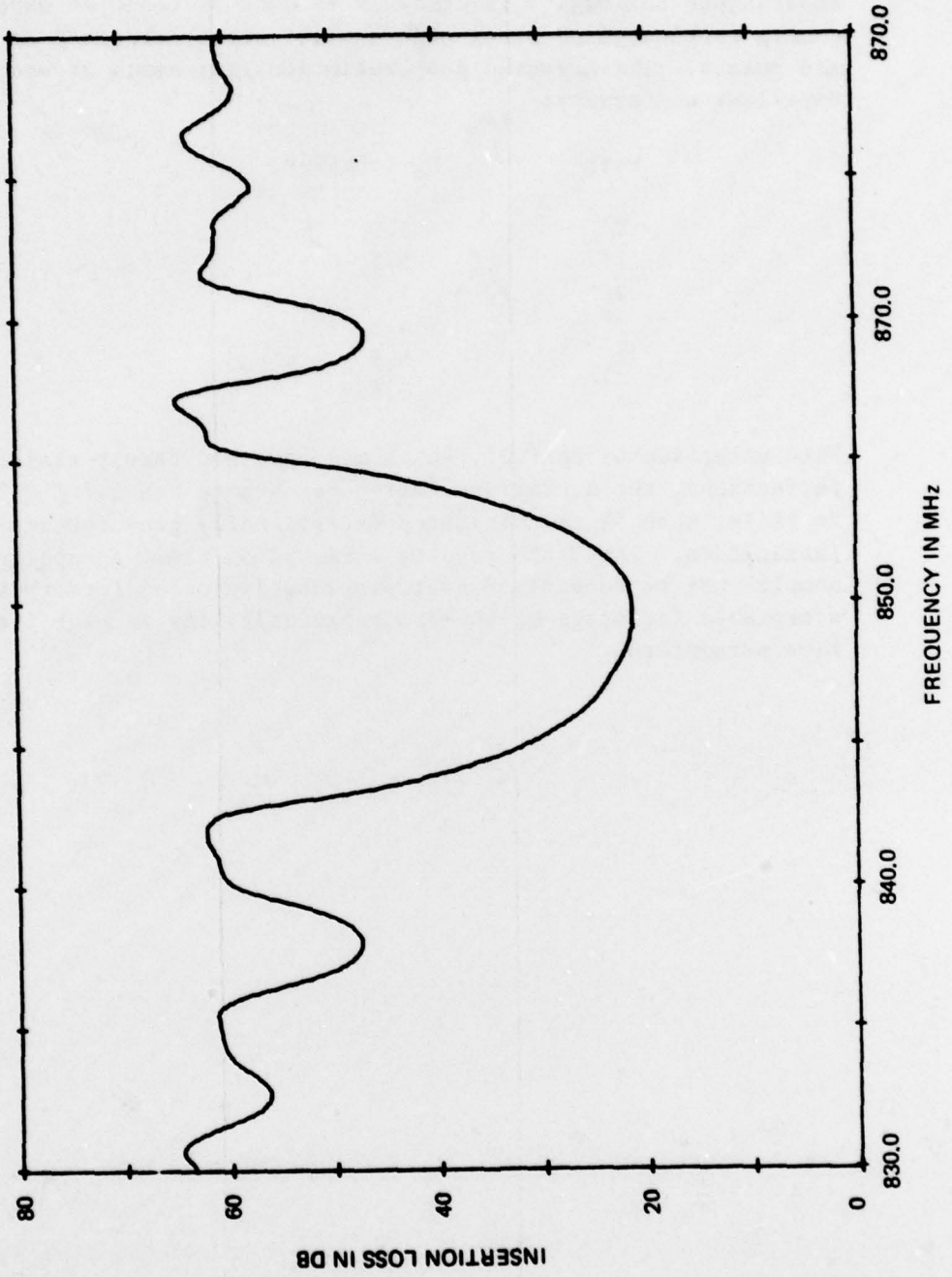

78-05-154-3

The transducers in M-521 used $\lambda_o/4$ electrodes with 3.0 μm width. The $\pm$ 5% capacitance uniformity is probably as good as could be expected from transducers fabricated on other high quality substrates such as lithium niobate and quartz. The measured peak radiation resistance at each port also showed excellent uniformity:

Port	R_a (ohms)
1	5.9
1'	5.5
2	5.7
2'	4.9
3	5.8
3'	5.8

With exception of port 2', which may have had barely visible electrode imperfections, the average radiation resistance was 5.7 $\pm$ 0.2 ohm. Uniformity to better than 5% is considered exceptionally good for small lot delay line fabrication. Thus, the results achieved on these as sputtered AlN/sapphire samples may be considered as representative of uniformity that would be quite acceptable for state-of-the-art reproducibility in high frequency SAW delay line parameters.

III. CONCLUSIONS AND RECOMMENDATIONS FOR FUTURE WORK

As stated earlier, the major goals of this program were to demonstrate that AlN films on sapphire prepared by rf reactive sputtering in an ammonia gas atmosphere could meet the following criteria:

1. film thickness - 2 to 8 microns
2. film thickness variation - within 0.1 microns across the long dimensions of a 25.4 x 9.0 x 2.0 mm (0001) oriented sapphire substrate
3. film quality - single crystal AlN films with optical surface quality.

1. Film Thickness

At a deposition rate of 70 Å/min, the deposition time required to deposit an AlN film of 2 μm is very nearly 5 hours. Since some time must be alloted for loading, start up and cool down, this means that 5 hours of deposition time is about the maximum amount of time which can be devoted to growing the film during a normal 8 hour work day. While it was indeed possible to grow AlN films slightly thicker than 2 μm conveniently in this program, in order to grow thicker films, further work should be done to increase the deposition rate while still maintaining other film qualities. Improvements in deposition rate may indeed be possible by changes in the sputtering geometry and operating conditions.

2. Film Thickness Variation

No difficulty was experienced in achieving film uniformity within 0.1 microns across the 25.4 mm length of the substrate. Typically the thickness variation was more nearly 0.05 micron across the sample. For a 2 μm thick film this represents a 2.5% thickness variation. Since the total thickness variation

is proportional to total film thickness, with the present growth geometry, we could expect that the film thickness variation could be held to 0.1 μm for film thickness up to 4 μm. Again, changes in sputtering geometry and conditions could be altered which could improve the thickness uniformity so that thicker more uniform films could be grown.

3. Film Quality

For as yet unexplained reasons, we have never been able to duplicate the crystalline quality of AlN films grown on the large thick (25.4 x 9.0 x 2.0 mm) substrates with those grown on the small thin (6 x 6 x 0.5 mm) substrates. While there was some variation in crystalline perfection among the films grown on the large thick substrates, none were of the very high quality consistently exhibited by the films grown on the small thin substrates. We can only speculate as to the reason for this discrepancy at this point, but one thought that does present itself is that the films on the thick substrate are more highly strained than the ones grown on the thin substrates. The reason for this is because some of the strain induced in the film during cool down is relieved by bowing of the thin substrate. However, the thick substrate is much more capable of resisting bowing and stresses the film to a much higher degree. During this program we have never experienced film cracking due to too rapid cool down with the thin substrates. However, we have seen cracking of several film samples on the thick substrates even when cool down was not considered to be particularly rapid.

Films grown on the large substrates are considered to be single crystal based on electron channeling and x-ray diffractometer analysis. However, it is felt that the reactive sputtering process is capable of producing films of higher crystalline perfection on the large substrates than what has been produced so far. Further work should also be done to improve this aspect of the process, since higher crystalline quality films should result in better piezoelectric properties.

One very positive result of growing the AlN films by sputtering is that no post deposition treatment of the films is necessary to improve their smoothness. Metallization patterns can be applied directly to the as-grown films.

The major item which contributed to reducing the yield of acceptable films was the presence of inclusions in the films. Since this is primarily a contamination problem, changes in the processing method could be found to improve the cleanliness.

4. SAW Piezoelectric Delay Line Performance

Surface acoustic wave transducers and delay lines were fabricated on selected AlN/sapphire samples in order to provide an estimate of the SAW piezoelectric and acoustic parameters for sputtered AlN on C-plane sapphire samples fabricated during this program. The fabrication of such devices and the work required to obtain these desirable acoustic data were not included in the program work statement. However, UTRC felt that such acoustic data could be very important for use in other projects underway under corporate program funding. Consequently, funds were made available from an ongoing UTRC corporate program on sputtered film coatings so that a limited number of AlN/sapphire samples could be fabricated and measured as SAW transducers and delay lines. This parallel corporate sponsored work yielded experimental delay lines operating at 201, 477, and 848 MHz.

The results of the above experimental AlN/sapphire delay line studies were extremely encouraging. The experimental devices exhibited an interdigital transducer capacitance about twice that of corresponding devices fabricated on popular crystalline quartz substrates along with a piezoelectric coupling factor (k^2) very close to that usually found for ST-X quartz. Wave propagation losses appeared to be relatively low, even at high frequency (848 MHz). Uniformity for transducers fabricated over extreme positions on the 25.4 x 9.0 mm AlN/sapphire substrates was exceptionally good; transducer capacitance and peak radiation resistance appeared to be uniform to 5% or better. Film-substrate surfaces were smooth enough to allow fabrication of 0.85 μm wide transducer electrodes; the excellent results obtained at 848 MHz utilized lines of this size. We conclude that it should be possible to fabricate high quality SAW filters on AlN/sapphire substrates like those studied here which could operate at center frequencies from 100 to 1000 MHz and perhaps to even higher frequencies.

5. Recommendations For Further Work

The results on sputtered AlN on sapphire achieved during this program prove that the sputtered film approach can provide high quality AlN/sapphire samples with optically smooth surfaces which are ready for device fabrication without resort to mechanical polishing as must be done with similar samples prepared by chemical vapor deposition (CVD). Moreover, the results obtained here appear to imply a better uniformity of acoustic parameters for transducers fabricated at widely separated points on a 25.4 x 9.0 mm substrate surface. On the other hand, the estimated piezoelectric coupling constant for films sputtered on C-plane sapphire are somewhat lower than coupling values achieved for CVD AlN on R-plane sapphire.

In our view, further detailed work should be carried out to find conditions for producing higher piezoelectric coupling constants for sputtered AlN/sapphire and to prove that specific designs of high quality bandpass filter structures can be built on sputtered AlN/sapphire surfaces. The results of such a further study would provide the information necessary to establish a firm basis for later development of this technology for the manufacturing of low cost, high frequency filters such as might be used for the man-pack version of the JTIDS military communication system. Because of its high SAW velocity (v ~ 5730 m/s, bandpass filters may be fabricated on sputtered AlN/sapphire using the superior $\lambda_o/8$ electrode transducer approach at center frequencies up to 1000 MHz. A significant advancement in the state-of-the-art of high frequency SAW filters could be achieved by a program which would show that sputtered AlN/sapphire will yield many (6-12) identical bandpass filters which are designed to operate at 1000 MHz with high skirt selecticity and highly reproducible insertion loss and center frequency parameters. Such a program would <u>not</u> require polishing of the AlN/sapphire surface before filter fabrication and therefore would be directed at what is most likely to be the most inexpensive and cost effective approach to the fabrication of truly high frequency SAW filters.

REFERENCES

1. Wauk, M. T. and D. K. Winslow: Appl. Phys. Lett., 13, 286 (1968).

2. Manasevit, H. M., F. M. Erdmann and W. R. Simpson: J. Electrochem. Soc., 118, 1864 (1971).

3. Duffy, M. T., C. C. Wang, J. D. O'Clock, Jr., S. H. McFarlane III, and P. J. Zangucchi: J. Electron. Mater., 2, 359 (1973).

4. Norieka, A. J., M. H. Francome and S. A. Zeitman: J. Fac. Sci. Technol., 6, 194 (1969).

5. Rutz, R. F., E. P. Harris and J. J. Cuomo: IBM J. Res. Develp. 17, 61 (1973).

6. Shuskus, A. J., D. J. Quinn, E. L. Paradis, J. M. Berak, D. E. Cullen, and T. M. Reeder: "Sputtered Thin Film Research," Fifth Semi-Annual Technical Report, November 1974, Contract N00014-72-C-0415.

7. Shuskus, A. J., T. M. Reeder and E. L. Paradis: Appl. Phys. Lett., 24, 155 (1974).

8. Laker, K. R., A. J. Budreau, and P. H. Carr: Proceedings of the IEEE (May 1976).

9. Paradis, E. L.: J. Vac. Sci., Technol., 11, 1170 (1974).

10. Pastrnak, J. and L. Roskovcova: Phys. Status Solidi, 14, K5 (1966).

11. Ott, H.: Z. Physik, 22, 201 (1924).

12. Stachelberg, M. V. and K. F. Spiess: Z. Phys. Chem., A175, 140 (1935).

13. Jeffrey, G. A. and G. S. Parry: J. Chem. Phys., 23, 406.

14. Kohn, J. A., P. G. Cotter and R. A. Potter: Am. Mineral, 41, 355 (1956).

15. ASTM X-Ray Powder Data File No. 8-262.

16. Taylor, K. M. and C. Lenie: J. Electrochem. Soc.,107, 308 (1960).

17. Yim, W. M. and R. J. Paff: J. Appl. Phys., 45, 1456 (1974).

18. Winters, H. F. and Eric Kay: J. Appl. Phys., 38, 3929 (1967).

REFERENCES

19. Smith, W. R., et. al.: IEEE Trans. on Microwave Theory & Tech., MTT-17, 856-864 (November 1969).

20. Smith, H. I.; Bachner, F. J. and N. Efremow: J. Electro-Chem. Soc., 118, 821-825 (May 1971).

21. Laker, K. R.: Budreau, A. J., and P. H. Carr: Proc. IEEE, 64, 692-695 (May 1976).

22. Reeder, T. M. and J. L. Swindal: Final Tech. Report on Contract DAAB07-73-C-0194, Section 4, U.S. Army Electronics Command, Ft. Monmouth, N.J. (November 1974).

23. Matthaei, G. L.; Wong, D. Y. and B. P. Shaughnessy: IEEE Trans. on Sonics and Ultrasonics, SU-22, 105-114 (March 1975).

24. Slobodnik, A. J.: IEEE Trans. on Sonics and Ultrasonics, SU-20, 315-323, (October 1973).

25. Bristol, T. W.: Proc. of the Int'l Specialist Seminar on Surface Acoustic Wave Devices, 115-129, IEEE Publ. No. 109 (September 1973).

26. Cullen, D. E., et al: Quarterly Status Report No. 2, Contract F19628-77-C-0244, RADC/ETEM, Hanscom AFB, Bedford, MA (March 1978).

MISSION
of
Rome Air Development Center

RADC plans and conducts research, exploratory and advanced development programs in command, control, and communications (C^3) activities, and in the C^3 areas of information sciences and intelligence. The principal technical mission areas are communications, electromagnetic guidance and control, surveillance of ground and aerospace objects, intelligence data collection and handling, information system technology, ionospheric propagation, solid state sciences, microwave physics and electronic reliability, maintainability and compatibility.

Printed by
United States Air Force
Hanscom AFB, Mass. 01731